# Stimulation of isoprene emissions and electron transport rates are a key mechanism of thermal tolerance in the tropical species *Vismia guianensis*

Running Title: Temperature, isoprene, and photochemistry

Tayana B. Rodrigues[1], Christopher R. Baker[2], Anthony P. Walker[3], Nate McDowell[4], Alistair Rogers[5], Niro Higuchi[1], Jeffrey Q. Chambers[1,6], Kolby J. Jardine[*1,6]

*[1.] Forest Management Laboratory, National Institute of Amazonian Research, Manaus, Amazonas, Brazil*
*[2.] Howard Hughes Medical Institute, Department of Plant and Microbial Biology, University of California, Berkeley, CA, USA*
*[3.] Environmental Sciences Division and Climate Change Science Institute, Oak Ridge National Laboratory, Oak Ridge, TN, USA*
*[4.] Earth System Analysis and Modeling, Pacific Northwest National Laboratory, Richland, WA, USA*
*[5.] Environmental and Climate Sciences Department, Brookhaven National Laboratory, Upton, NY, USA*
*[6.] Climate and Ecosystem Sciences Division, Lawrence Berkeley National Laboratory, Berkeley, CA, USA*
*Author for correspondence:
Kolby Jardine
Tel: (510) 495-8231
Email: kjjardine@lbl.gov

| Total word count (excluding summary, references and legends): | 6,661 | N° of figures: | 6 (all in color) |
|---|---|---|---|
| Summary: | 285 | N° of tables: | 1 |
| Introduction: | 2,036 | | |
| Material and Methods: | 1,548 | | |
| Results: | 1,038 | | |
| Discussion: | 1,934 | | |
| Acknowledgements | 105 | | |

**Summary**

Tropical forests absorb large amounts of atmospheric $CO_2$ through photosynthesis, but high surface temperatures suppress this absorption while promoting isoprene emissions. While mechanistic isoprene emission models predict a tight coupling to photosynthetic electron transport (ETR) as a function of temperature, direct field observations of these phenomenon are lacking in the tropics and are necessary to assess the impact of a warming climate on global isoprene emissions. Here, we demonstrate that in the early successional species *Vismia guianensis* in the central Amazon, ETR rates increased with temperature in concert with isoprene emissions, even as stomatal conductance ($g_s$) and net photosynthetic carbon fixation ($P_n$) declined. We observed the highest temperatures of continually increasing isoprene emissions yet reported (50°C). While $P_n$ showed an optimum value of 32.6 ± 0.4°C, isoprene emissions, ETR, and the oxidation state of PSII reaction centers ($q_L$) increased with leaf temperature with strong linear correlations for ETR ($p$ = 0.98) and $q_L$ ($p$ = 0.99) with leaf isoprene emissions. In contrast, other photoprotective mechanisms, such as non-photochemical quenching (NPQ), were not activated at elevated temperatures. Inhibition of isoprenoid biosynthesis repressed $P_n$ at high temperatures through a mechanism that was independent of stomatal closure. While extreme warming will decrease $g_s$ and $P_n$ in tropical species, our observations support a thermal tolerance mechanism where the maintenance of high photosynthetic capacity under extreme warming is assisted by the simultaneous stimulation of ETR and metabolic pathways that consume the direct products of ETR including photorespiration and the biosynthesis of thermoprotective isoprenoids. Our results confirm that models which link isoprene emissions to the rate of ETR hold true in tropical species and provide necessary "ground-truthing" for simulations of the large predicted increases in tropical isoprene emissions with climate warming.

***Key words***: *global warming, high temperature stress, leaf gas exchange, chlorophyll fluorescence, fosmidomycin, electron transport rates, net photosynthesis, isoprene energetic requirements*

## 1. Introduction

Tropical forests absorb large amounts of atmospheric $CO_2$, accounting for an estimated ~34% (42 Pg C $yr^{-1}$) of global terrestrial gross primary production (Beer *et al.*, 2010). However, substantial decreases in tropical forest gross primary productivity have been repeatedly demonstrated in the Amazon basin during periodic widespread drought associated with high temperature (Potter *et al*. 2011; Liu *et al.*, 2017). Therefore, the physiological mechanisms through which tropical forests respond to high temperature are critically important to understand. One such mechanism is the biosynthesis and emission of the volatile organic compound isoprene ($C_5H_8$), which can act as a thermotolerant and may be associated with stress protection at elevated temperatures (Jardine *et al*. 2017, Sharkey and Yeh 2001).

During photosynthesis, energy from absorbed light is dissipated by three processes: photochemistry, chlorophyll fluorescence, and thermal dissipation (measured as non-photochemical quenching, NPQ). The relative contribution of these three processes to total energy dissipation is highly sensitive to leaf temperature (Müller *et al.*, 2001). Chlorophyll fluorescence is light emitted at wavelengths centered on 682 nm or 740 nm (Krause & Weis, 1984) and changes in fluorescence and derived photochemical parameters during high leaf temperatures have been widely used to provide insight into photochemical metabolism (Li *et al.*, 2009). For example, variable chlorophyll fluorescence (Fv), is the difference between the maximum (Fm) and minimum fluorescence (Fo). Decreases in the ratio (Fv/Fm) of variable (Fv) to maximum (Fm) chlorophyll fluorescence have been widely used to demonstrate environmental stress effects on the quantum

efficiency of Photosystem II (Murchie and Lawson 2013). During the 2015/2016 El Niño Amazon drought, sun-induced fluorescence, a metric of gross primary productivity, was strongly suppressed over areas with anomalously high temperatures and decreased levels of soil moisture (Koren *et al.*, 2018). Elevated leaf temperatures strongly enhance leaf-to-atmosphere vapor pressure deficits which drives high leaf transpiration rates and reductions in plant water potentials. To avoid excessive water loss and hydraulic failure, an afternoon reduction in stomatal conductance ($g_s$) is often observed, resulting in an afternoon depression of $P_n$ during warm afternoons (Koch *et al.*, 1994; Chambers & Silver, 2004). In the Tapajos National Forest in east-central Amazon, a corresponding mid-day and post mid-day depression in net ecosystem exchange of $CO_2$ was regularly observed using eddy covariance (Piedade *et al*., 1994; Goulden *et al*., 2004).

It has been hypothesized that reductions in $P_n$ at high leaf temperatures in tropical species, are mainly associated with reductions in $g_s$ rather than direct negative temperature effects on photosynthetic electron transport, or the light-independent reactions of photosynthesis (Lloyd & Farquhar, 2008). However, few experimental observations in the tropics have evaluated these hypotheses, especially in early successional species that tend to show high rates of $P_n$. The Neotropical early successional genera *Vismia* dominates large rainforest disturbance gaps in the Amazon Basin (Chambers *et al*., 2009) where it helps accelerate the regeneration of secondary forests by influencing forest successional pathways (Uhl *et al*., 1988; Zalamea & González, 2008; Brienen *et al*., 2015). The establishment of early successional genera in secondary forests is related to their ability to maintain high $P_n$ and growth under conditions of full sunlight and high leaf temperatures characteristic of tropical landscapes impacted by natural (Chambers *et al*., 2009) and human (Mesquita *et al*., 2015) disturbances. *Vismia* leaves show high rates of isoprene emissions (Jardine *et al*., 2016), which is hypothesized to play an important role in thermotolerance of

98 photosynthesis (Singsaas *et al*., 1997; Sharkey *et al.*, 2001; Sharkey, 2005; Sasaki *et al*., 2007). As
99 previously reviewed (Harley *et al.*, 1999), stimulation of isoprene production by high irradiance
100 and warm temperatures is consistent with physiological evidence of a role in ameliorating stresses
101 associated with warm and high-light environments.

102 Plants utilize the products of both the light (ATP and NADPH) and light-independent
103 reactions of photosynthesis to synthesize a number of photosynthetic components and defense
104 compounds via the isoprenoid pathway in chloroplasts (Lichtenthaler, 1987; Affek & Yakir, 2003).
105 Tropical ecosystems are recognized as the largest source of isoprene emissions to the atmosphere,
106 representing roughly half of the estimated global annual emissions of 440-660 Tg C $yr^{-1}$ (Guenther
107 *et al.*, 2006). Isoprene biosynthesis begins with the initial condensation of pyruvate and
108 glyceraldehyde-3-phosphate derived from the Calvin-Benson-Bassham cycle (Silver & Fall,
109 1995). Leaf isoprene emissions are strongly stimulated by temperature (Duncan *et al.*, 2009) with
110 global emission models predicting future increases in tropical forest isoprene emissions and their
111 corresponding impacts on atmospheric chemistry and climate including altering the dynamics and
112 lifetimes of atmospheric oxidants, secondary organic aerosols, and cloud condensation nuclei
113 (Pacifico *et al.*, 2009). Isoprene emissions from terrestrial plants are completely dependent on
114 illumination (Sanadze, 1991), including tropical trees (Jardine *et al.*, 2014), consistent with the
115 view that the isoprenoid pathway is completely dependent on photosynthetic electron transport
116 (Lantz *et al.*, 2019).

117 While the mechanisms of isoprene thermotolerance are under investigation, recent
118 literature suggests that isoprene and other isoprenoids protect photosynthesis during abiotic stress
119 by minimizing oxidative damage through a number of mechanisms including; physical
120 stabilization of photosynthetic membranes, the consumption of photosynthetic energy and

121 reducing equivalents, direct antioxidant reactions (e.g. between isoprene and reactive oxygen
122 species including fatty acid peroxyl radicals), and potent phytohormone signaling properties of
123 isoprene including oxidation products methyl vinyl ketone and methacrolein which activate
124 defense gene expression (Singsaas *et al.*, 1997; Velikova *et al.*, 2008; Vickers *et al.*, 2009a, 2009b;
125 Karl *et al.*, 2010; Jardine *et al.*, 2012; Morfopoulos *et al.*, 2014, Junker-Frohn *et al*., 2019, Zuo *et*
126 *al.,* 2019). For example, in *Populus nigra* and *Phragmites australis* leaves exposed to oxidative
127 stress, reduced damage to photosynthesis, accumulation of $H_2O_2$, and membrane denaturation was
128 attributed, in part, to isoprene production (Velikova *et al.*, 2008). However, there is limited
129 evidence for the occurrence of these mechanisms in the tropics where field data are scarce.

130 Leaf isoprene emissions are generally assumed to account for 1–2% of $P_n$ at leaf
131 temperatures below the optimum for $P_n$, but have been reported to represent 10% of $P_n$ or higher
132 at temperatures above the optimum (Harley *et al.*, 1996). While $P_n$ in tropical trees generally have
133 an optimum leaf temperature between 28 - 32°C, emissions of isoprene at the leaf level have been
134 consistently shown to continue to increase up to 40°C or beyond (Alves *et al.,* 2014; Jardine *et al.,*
135 2014, 2017a). Observations at ecosystem scales in the tropics observed the highest isoprenoid
136 emission fluxes during the hottest period of the day (12:00h–14:00h) when $g_s$ and $P_n$ are reduced
137 (Karl *et al.,* 2009; Jardine *et al.,* 2011, 2017a). Therefore, the increasing importance of isoprene
138 emissions to plant carbon budgets under high temperatures is recognized as a consequence of both
139 the stimulation of isoprene emissions and the suppression of $P_n$ (Monson *et al.*, 1992). $^{13}CO_2$
140 labeling revealed that under optimal conditions of $P_n$, 70 - 90% of the carbon used for isoprene
141 synthesis is produced from recently assimilated atmospheric $CO_2$ (Delwiche & Sharkey, 1993;
142 Affek & Yakir, 2003). In contrast, under high leaf temperatures and drought conditions where $P_n$
143 is suppressed, isoprene carbon sources have been shown to increasingly derive from previously

144 assimilated or stored carbon (Funk *et al*., 2004). While a number of extrachloroplastic metabolites
145 have been considered as 'alternate' carbon including pyruvate, glucose, acetate, and the $C_1$
146 pathway (Jardine *et al.*, 2010, 2017b; Kreuzwieser *et al.*, 2002, de Souza *et al*., 2018), evidence
147 using $^{13}C$-labeled photorespiratory intermediates and $CO_2$-free atmospheres suggest that re-
148 assimilation of internal plant sources of $CO_2$ like photorespiration, respiration, and xylem-
149 transported $CO_2$ may help explain this 'alternate' carbon source for isoprene and contribute to the
150 suppression of $P_n$ at high temperatures (Jardine *et al*., 2014, 2017a; Garcia *et al*., 2019; Guidolotti
151 *et al.,* 2019). This is consistent with the recent observation that the majority of xylem-transported
152 $CO_2$ is re-assimilated in illuminated leaves (Stutz & Hanson, 2019).

153 In addition to strong uncoupling between isoprene emissions and $P_n$ at high temperature,
154 elevated $CO_2$ has been widely reported to stimulate $P_n$ while suppressing isoprene emissions
155 (Loreto & Sharkey, 1993). While various mechanisms including a key role of extrachloroplastic
156 intermediates have been discussed in the literature, recent evidence suggests that the elevated $CO_2$
157 effect is largely driven by a limited supply of energetic and reductive equivalents for isoprenoid
158 biosynthesis generated by the photochemical phase of photosynthesis (Rasulov *et al.*, 2009, 2018;
159 Morfopoulos *et al.*, 2014). In 2002, strong positive correlations was first described between foliage
160 isoprenoid emissions and photosynthetic electron transport rates (ETR) in the Mediterranean trees
161 *Quercus coccifera* and *Q. ilex* (Niinemets *et al.*, 2002a) and an early model was developed
162 discussing light-dependent NADPH limitation of isoprenoid leaf emissions (Niinemets *et al.*,
163 2002b). Following these initial discoveries and developments, positive linear correlation between
164 ETR and isoprene emissions were observed at elevated $CO_2$ mixing ratios in both *Quercus*
165 *pubescens* and *Quercus ilex* (Rapparini *et al.*, 2004), and later a model was developed showing
166 NADPH limitation of isoprene emissions under different light, leaf intercellular $CO_2$

concentrations ($C_i$) and temperature conditions (Morfopoulos *et al.*, 2013). A similar model was then used to explain how the elevated $CO_2$ enhancement of $P_n$, but suppression of isoprene emission, is driven by a limited supply of NADPH for isoprenoid biosynthesis (Morfopoulos *et al.*, 2014), and these mechanisms were extended to include drought effects where increased isoprene emissions are maintained due to the increased ratio of ETR to $P_n$. (Dani *et al.*, 2015).

Using post-illumination isoprene bursts to estimate the pool size of the isoprene precursor dimethylallyl diphosphate (DMADP) in oak (*Quercus robur*) and poplar (*Populus deltoides*) leaves, DMADP was observed to increase with temperature up to 35°C (Li *et al.*, 2011). ETRs in many plants generally demonstrate higher optimum leaf temperatures than $P_n$ under current atmospheric $CO_2$ concentrations (Ishida & Toma, 1999; Himalayan & Tech, 2005; Sage & Kubien, 2007) and isoprene energetic models predict a temperature optimum of isoprene emissions that closely follows the temperature optimum of ETR (a temperature optimum higher than $P_n$ but lower than that of isoprene synthase activity) (Morfopoulos *et al.*, 2013). Thus, there is considerable evidence that the rate-limiting steps for isoprenoid biosynthesis *in vivo* depends on the availability of NADPH and ATP in the chloroplast, the direct products of ETR (Rasulov *et al.*, 2009, 2018). Unfortunately, studies with parallel measurements of ETR and isoprene emissions as a function of temperature are relatively rare and experimental data on abundant tropical species at high temperature is lacking.

Here we hypothesize that in early successional tropical species high temperatures will be associated with an enhanced rate of production of the energetic and reductive equivalents necessary for isoprenoid biosynthesis and generated by the photochemical phase of photosynthesis. Thus, in spite of reduced $P_n$ at high temperatures, ETR will continue to increase at elevated temperatures together with high isoprenoid biosynthesis rates and other chloroplastic

190 NADPH/ATP consuming pathways such as photorespiration (Voss *et al.*, 2013), thereby limiting
191 rates of NPQ at high temperatures. We also hypothesize that inhibition of isoprenoid biosynthesis
192 would reduce $P_n$ at high temperatures both due to the direct loss of the thermoprotective role of
193 isoprene as well as the potential antioxidant and signaling roles of isoprene. We test these
194 hypotheses by quantifying the suppression of $P_n$ and $g_s$ at high leaf temperatures together with
195 changes in photochemical parameters of photosynthesis and isoprene emissions in the fast growing
196 early successional species *Vismia guianensis* (Aubl.) Pers in the central Amazon. We combine gas
197 exchange during leaf temperature response curves with chlorophyll fluorescence and isoprene
198 emissions, and therefore simultaneously characterize the temperature sensitivities of $P_n$, $g_s$,
199 isoprene emissions, and key parameters of the photochemical reactions of photosynthesis
200 including ETR, non-photochemical quenching (NPQ), the oxidation state of PSII reaction centers
201 ($q_L$), and the maximum quantum efficiency of PSII in the dark (Fv/Fm) and light (Fv'/Fm').
202 Further, by delivering a specific inhibitor of the isoprenoid pathway (fosmidomycin) to
203 detached *V. guianensis* branches, we evaluate the impact of blocking isoprenoid production on $P_n$
204 at high leaf temperatures. We discuss the results in terms of thermotolerance mechanisms in
205 tropical plants including the role of isoprene may have in supporting the upregulation of ETR
206 rather than NPQ at high leaf temperatures. Finally, we discuss the implications for modeling of
207 future isoprene emissions from tropical forests and interpretation of remote sensing studies
208 tracking seasonal patterns in regional isoprene emissions, gross primary productivity, and canopy
209 temperature.
210
211 **2. Materials and Methods**
212 **2.1 Site description**

213 Coupled gas-exchange and chlorophyll fluorescence measurements were carried out on
214 three individuals of *V. guianensis* (Aubl.) Pers., an early successional tree species from the
215 Hypericaceae family. Four *V. guianensis* individuals were studied in the Reserva Biológica do
216 Cuieiras (ZF2), a primary rainforest biological reserve located approximately 60 km northwest of
217 Manaus, in the central Amazon Basin, Brazil (Higuchi *et al.*, 1998). The *V. guianensis* individuals
218 ranged between 1.6 m and 2.0 m in height and were exposed to full sunlight conditions throughout
219 a large part of the day due to their presence in gap associated with the site access road.

220 **2.2 Gas exchange data**

221 The coupled leaf isoprene emissions, gas exchange, and chlorophyll fluorescence field
222 measurements were made during October 2017 and April, May, June, July, and August of 2018.
223 For each of the four *V. guianensis* individuals, 2-8 leaf temperature response curves were
224 conducted between 7:00-15:00 (23 total response curves, 1-3 per day). All leaves selected for study
225 were dark green and considered developmentally and physiologically mature, with no obvious
226 visual problems and little herbivory. Previous research has shown that mature *V. guianensis* leaves
227 in the central Amazon showed substantially higher rates of $P_n$, isoprene emissions, and $g_s$ under
228 standard environmental conditions than young, rapidly expanding light green leaves (Jardine *et*
229 *al*., 2016).

230 Gas exchange responses to leaf temperature for *V. guianensis* leaves were collected in the
231 field using a portable photosynthesis system with a 2 $cm^2$ leaf fluorescence chamber (6400XT,
232 Licor Biosciences) adapted for the collection of isoprene emissions by the diversion of a fraction
233 (100 ml $min^{-1}$) of the air sample leaving the leaf chamber through a clean thermal desorption tube
234 packed with Quartzwool, Tenax TA and Carbograph 5TD adsorbents (Markes International) for
235 10 min using a hand-held pump (APEX, Casella, USA) (Jardine *et al.*, 2015b). Each leaf placed in

236 the chamber was maintained under constant photosynthetically active radiation (PAR) of 0 μmol
237 $m^{-2}$ $s^{-1}$ for the dark temperature response curve. In a previous study at constant leaf temperature
238 (30°C) we showed that during both the wet and dry seasons, developmentally and physiologically
239 mature *V. guianensis* leaves reached light saturation of $P_n$ at PAR fluxes between 750-1000 μmol
240 $m^{-2}$ $s^{-1}$ (Jardine *et al*., 2016). Thus, we chose to conduct all leaf temperature response curves in
241 the wet and dry seasons under the standard PAR flux of 1000 μmol $m^{-2}$ $s^{-1}$, which also facilitates
242 future modeling studies requiring the standard isoprene emission potential parameter, defined as
243 the emissions under 30°C and 1000 μmol $m^{-2}$ $s^{-1}$ PAR. Throughout temperature response curves in
244 the dark and light, the reference $CO_2$ concentration was maintained at 400 ppm, and air flow rate
245 entering the leaf chamber was held constant at 400 μmol $s^{-1}$. Once the leaf was placed in the
246 chamber at 0 μmol $m^{-2}$ $s^{-1}$ PAR, a black cloth was used to cover the chamber. Following a 15 min
247 period of leaf dark adaption, the dark leaf temperature response curve was initiated to demonstrate
248 the lack of isoprene emissions in the dark and to acquire the dark parameters of chlorophyll
249 fluorescence. Following the completion of the dark temperature response curve, the black cloth
250 was removed, the PAR was set at 1000 μmol $m^{-2}$ $s^{-1}$. Following a period of light adaptation required
251 to reach steady state gas exchange (10-40 min), the temperature response curve of the illuminated
252 leaf was initiated. Leaf temperature response curves were generated by setting the block
253 temperature to 25, 27.5, 30.0, 32.5, 35, 37.5, 40, and 42.5 ºC, sequentially. The leaf temperature
254 was directly measured using a leaf thermocouple mounted inside the leaf chamber.
255
256 **2.3 Chlorophyll Fluorescence**
257 For all leaves studied during October 2017 and April, May, June, July, and August of 2018,
258 a leaf chamber fluorimeter (LCF 6400-40, Licor Biosciences) was used to simultaneously quantify
259 leaf gas exchange and chlorophyll fluorescence. The fluorimeter was unavailable during the

isoprenoid inhibition experiments which occurred earlier during the July 2017 (see **section 2.5**). Following leaf acclimation to each successive temperature increase, an actinic light pulse of 7,000 μmol $m^{-2}$ $s^{-1}$ (10% blue light and 90% red light), modulated at 20 KHz, was applied for 1 sec and the average chlorophyll fluorescence signal was recorded. The average chlorophyll fluorescence signal at each leaf temperature was used to determine minimum fluorescence (Fo), maximum fluorescence (Fm), and steady-state fluorescence (Fs). Derived photochemical parameters at each leaf temperature were calculated according to **Eqs. 1-5** where derived parameters with prime, for example Fo`, are values related to the data in the light and those with no prime corresponding to data from the dark adapted leaf (Baker & Rosenqvist, 2004).

The electron transport rate (ETR, μmol $e^-$ $m^{-2}$ $s^{-1}$) was calculated according to **Eq. 1**, where f is the fraction of the quantum absorbed and used by Photosystem II, with a value of 0.5 used for $C_3$ plants (Earl & Tollenaar, 1998), PAR is incident photon flux density, and $\alpha_{leaf}$ is leaf absorbance (0.87).

**Eq. 1.** $ETR = \left(\frac{Fm` - Fs}{Fm`}\right) f \cdot PAR \cdot \alpha_{leaf}$

The redox state of $Q_A$, the primary electron accepter of PSII, was determined by quantification of the photochemical extinction coefficient ($q_L$) according to **Eq. 2**. $q_L$ is an estimate of the average oxidation level of PSII reaction centers. which is a measure of the fraction of $Q_A$ in an oxidized state (Kramer & Johnson, 2004). Thus, an increase in $q_L$ indicates that average oxidation level of PSII increased to support, for example, an upregulation of ETR, NADPH/ATP production, and isoprenoid biosynthesis.

**Eq. 2.** $qL = \frac{\frac{1}{Fs} - \frac{1}{Fm'}}{\frac{1}{Fo'} - \frac{1}{Fm'}}$

Photon capture efficiency of photosynthetic reaction centers in the light was estimated according to **Eq. 3**.

**Eq. 3.** Maximum quantum efficiency of PSII photochemistry of dark adapted leaves: $\frac{Fv}{Fm}$, and light adapted leaves: $\frac{Fv'}{Fm'}$

Finally, we estimated non-photochemical quenching (NPQ) according to **Eq. 4**.

**Eq. 4.** $NPQ = \frac{Fm - Fm`}{Fm`}$

Immediately following the chlorophyll fluorescence measurements, isoprene emissions were collected on a single thermal desorption tube for 10 minutes while gas exchange data were logged simultaneously on the Li6400XT.

**2.4 Leaf isoprene emissions**

Following sample collection in the field, the thermal desorption tubes were transported to the laboratory in Manaus, Brazil, for the analysis of adsorbed isoprene using an automated thermal desorption system (TD-100, Thermal Desorber, Markes International, UK) coupled to a gas chromatograph (series 7890A, Agilent Technologies, USA) and mass spectrometer (Agilent ChemStation, Agilent Technologies, USA) (TD-GC-MS) installed at the National Research Institute of the Amazon (INPA) (Jardine *et al.*, 2015a). The system was calibrated for isoprene using m/z 67 as the most abundant ion formed during electron impact ionization as previously described (Jardine *et al.*, 2016). The average leaf isoprene emission rate (nmol $m^{-2}$ $s^{-1}$) at each leaf temperature was calculated according to **Eq. 6** where PA67 is the GC-MS peak area at the retention time for isoprene (ion counts of m/z 67 x min), Cal is the calibration factor determined for isoprene ($10^{-6}$ nL isoprene/peak area), F is the flow rate of air into the leaf chamber (400 µmol $s^{-1}$), $10^{-6}$ is the factor used to convert µmoles to moles, $Leaf_{Area}$ is the leaf area enclosed in the chamber of 0.0002 $m^2$, and Volume is the total volume of air that passed through the thermal desorption tube (1.0 L).

306 **Eq. 6**. $Isoprene\ emission = PA67 \times Cal \times F \times 10^{-6}/(Leaf_{Area} * Volume)$

307

308 **2.5 Inhibition of the isoprenoid pathway with fosmidomycin**

309 In a separate experiment during July and August of 2017, we inhibited the production of
310 leaf isoprene in *V. guianensis*, by feeding excised branches with 12.5 mM fosmidomycin. Branches
311 were cut between 8:00h-8:30h and then immediately recut under either water (control, 4 branches,
312 1 branch per individual) or the fosmidomycin solution (3 branches, 1 branch per individual) and
313 allowed to transpire for 1h in full sunlight in order to ensure delivery of the inhibitor to the leaves.
314 Previous work has shown that a low concentration of fosmidomycin (4 μM) delivered to leaves of
315 mid-latitude species was sufficient to inhibit leaf isoprene emissions (Sharkey & Yeh, 2001).
316 However, in our study we found that 12.5 mM fosmidomycin solution was required to completely
317 inhibit production of leaf isoprene in *V. guianensis*. Following inhibitor uptake, the temperature
318 response curves of gas exchange and isoprene emissions were measured as described above with
319 the exception that we used the standard 6 $cm^2$ leaf chamber with red and blue LED light source
320 (6400-02B, Licor Biosciences, USA). Note that in the inhibitor experiments with detached
321 branches, we were able to achieve higher leaf temperatures due to direct solar heating of the
322 chamber because of cloud free conditions during the 2017 dry season.

323 **2.6 Statistical Analysis**

324 Statistical analysis of the 23 leaf temperature response curves included calculating the mean
325 and confidence interval (± 2 standard deviation) of the leaf temperature, gas exchange
326 characteristics (e.g. $P_n$ and $g_s$), photochemical characteristics (e.g. ETR, qL, Fv'/Fm', and NPQ),
327 and isoprene emissions at each block temperature. Pearson product-moment correlation
328 coefficients were determined between each possible pair of mean gas exchange and photochemical
329 variables together with mean isoprene emissions (**Table 1**). Linear coefficients of determination

330 ($R^2$) and the equations were determined during regression analysis between isoprene emissions
331 and the photochemical parameters ETR and $q_L$.
332 For the isoprenoid inhibitor experiments where gas exchange and isoprene emissions were
333 collected from 4 water-fed control branches and 3 inhibitor-fed branches, the mean and confidence
334 interval (± 2 standard deviation) calculations were made as a function of leaf temperature for $P_n$,
335 $g_s$, $C_i$, and isoprene emissions.

336

337 **3. Results**

338 **3.1 Gas exchange and photochemical parameters**

339 **Figures 1-2** show mean (± 2 standard deviations) gas exchange and photochemical
340 parameters as a function of mean leaf temperature. As leaf temperature increased from the lowest
341 value of 26.7 ± 0.5°C to 32.6 ± 0.4°C, net photosynthesis ($P_n$) and transpiration (E) were stimulated
342 to maximum values of 10.2 ± 1.1 μmol $m^{-2}$ $s^{-1}$ and 3.9 +/- 0.5 mmol $m^{-2}$ $s^{-1}$, respectively. As leaf
343 temperatures continued to increase from 32.6 ± 0.4 °C to the highest value (38.3 ± 0.4°C), $P_n$
344 decreased by 16% and reached a minimum of 8.6 ± 1.9 μmol $m^{-2}$ $s^{-1}$, while E decreased by 21% to
345 3.1 +/- 0.9 mmol $m^{-2}$ $s^{-1}$. In contrast, $g_s$ continuously decreased as leaf temperature increased. At
346 the lowest leaf temperature of 26.7 ± 0.5°C, $g_s$ was at a maximum value of 0.21 ± 0.05 mol $m^{-2}$ $s^{-}$
347 $^{1}$, while at 38.3 ± 0.4°C, $g_s$ reached a minimum value of 0.09 ± 0.04 mmol $m^{-2}$ $s^{-1}$, representing a
348 57% decline. Similarly, intracellular $CO_2$ ($C_i$) levels decreased linearly with leaf temperature,
349 which is consistent with the decline in $P_n$ being driven by the reduction in $g_s$ as opposed to a decline
350 in photosynthetic capacity (**Fig. 1**).
351 Together with isoprene emissions, two of the photochemical parameters (ETR and $q_L$)
352 associated with the light reactions of photosynthesis (**Fig. 2**) were strongly stimulated by
353 increasing temperatures with no sign of saturation or decline. A minimum ETR value of 123.1 ±

354 24.5 μmol $e^-$ $m^{-2}$ $s^{-1}$ occurred at the lowest leaf temperature (26.7 ± 0.5°C) and continuously
355 increased with leaf temperature to reach a maximum value of 189.4 ± 34.2 μmol $e^-$ $m^{-2}$ $s^{-1}$ at the
356 highest leaf temperature (38.3 ± 0.4°C), representing a 54% increase. Similarly, over the same
357 temperature range, $q_L$ increased by 39% from 0.39 ± 0.06 at the lowest leaf temperature to 0.54 ±
358 0.05 at the highest leaf temperature, demonstrating that the average oxidation level of PSII
359 increased consistently as leaf temperature increased. Together with these photochemical
360 parameters, leaf isoprene emissions were strongly stimulated by increases in leaf temperature by
361 490% over the temperature range studied. Isoprene emissions were at a minimum of 6.1 ± 1.9 nmol
362 $m^{-2}s^{-1}$ at the lowest leaf temperature and increased to maximum emission rate of 29.9 ± 3.8 nmol
363 $m^{-2}s^{-1}$ at the highest leaf temperature. In contrast, NPQ was variable and did not show any clear
364 trend with leaf temperature; NPQ was 1.17 ± 0.60 at the lowest leaf temperature and 1.32 ± 0.81
365 at the highest leaf temperature (**Fig. 2**). In addition, Fv'/Fm' remained stable as leaf temperatures
366 increased with a variation of less than 1%, with a value of 0.57 ± 0.02 at the lowest leaf temperature
367 and 0.58 ± 0.05 at the highest leaf temperature (supplementary data, **figure S1**).

368 As summarized in **Table 1**, strong positive correlations (indicated with Pearson's product-
369 moment correlation coefficient, *r*) were observed between leaf isoprene emissions and $q_L$ and ETR.
370 Across the leaf temperature response curves, mean isoprene emissions were nearly perfectly
371 linearly correlated with mean values of ETR (r = 0.98) and qL (r = 0.99). In contrast, leaf isoprene
372 emissions were strongly negatively correlated with $g_s$ (r = -0.97) and $C_i$ (r = -0.97). Following
373 regression analysis, linear equations and coefficients of determination ($R^2$) were determined
374 between isoprene emissions and the photochemical parameters ETR (μmol $e^-$ $m^{-2}$ $s^{-1}$) and $q_L$ as
375 follows:

376 **Eq.7**. Isoprene emissions = (0.37 ± 0.03) ETR - 49.1 ± 4.19 ($R^2$ = 0.97)

377 **Eq.8.** Isoprene emissions = (126.26 ± 6.57) $q_L$ + 38.875 ± 2.89 ($R^2$ = 0.98)

378 **3.2 Isoprene inhibitor studies**

379 In order to test whether the isoprenoid pathway is necessary to maintain high
380 photosynthetic rates at elevated temperatures, we applied the isoprenoid biosynthesis inhibitor
381 fosmidomycin to detached branches as a solution delivered to leaves via the transpiration stream.
382 Fosmidomycin application resulted in the complete loss of isoprene emissions at all leaf
383 temperatures (**Fig. 3a**). In contrast, under water fed control branches, leaf isoprene emission
384 continued to be stimulated through the highest leaf temperatures achievable (47.9 ± 2.0°C). It
385 should be noted, that because the inhibitor experiments occurred during the dry season with greatly
386 reduced cloud cover, the maximum leaf temperatures achievable were much higher than in the
387 chlorophyll florescence experiments (**Figs. 1-2**), which occurred during the wet season with a
388 greater degree of cloud cover. Fosmidomycin treated branches showed reduced $g_s$ relative to water
389 fed controls (**Fig. 3d**). This reduction of $g_s$ caused a temperature independent reduction in $P_n$ in the
390 fosmidomycin treated leaves, reducing the values by up to 40% relative to the water fed control
391 (**Fig. 3b**). However, for both water fed control and fosmidomycin treated leaves, both $g_s$ and $P_n$
392 reached steady state at each temperature throughout the leaf temperature response curve.
393 Moreover, clear temperature dependent trends can be discerned from this dataset. For instance, at
394 the lowest leaf temperature (25.4 ± 1.2°C), mean $P_n$ of fosmidomycin fed branches decreased by
395 64% relative to water controls (14.3 ± 3.8 μmol $m^{-2}$ $s^{-1}$ under water versus 5.2 ± 1.1 μmol $m^{-2}$ $s^{-1}$
396 under fosmidomycin), while at the highest leaf temperature studied (47.9 ± 2.0°C) mean $P_n$ of
397 fosmidomycin fed branches decreased by 82.8% relative to water controls (8.7 ± 1.5 μmol $m^{-2}$ $s^{-1}$
398 versus 1.5 ±1.1 μmol $m^{-2}$ $s^{-1}$ under fosmidomycin). Intercellular $CO_2$ concentrations ($C_i$, **Fig. 3c**)
399 were similar between the fosmidomycin fed branches and the water fed controls at low leaf

400 temperatures, however, they diverged at leaf temperatures above 32.5°C. Above these leaf
401 temperatures, $C_i$ values of fosmidomycin fed branches were higher than water fed controls in spite
402 of the low $g_s$ values, consistent with reduced photosynthetic capacity (**Fig. 3b**). Finally, when $P_n$
403 was normalized by $g_s$, the temperature dependent effect of the inhibitor on photosynthesis can be
404 clearly observed ($P_n/g_s$, **Fig. 4**). At low temperatures, $P_n/g_s$ was indistinguishable between the
405 water fed control branches and the fosmidomycin fed branches (25.4 ± 1.2°C). At high
406 temperatures, $P_n/g_s$ was lower in the fosmidomycin fed branches relative to the water fed controls
407 as leaf temperature increased. The largest reduction in $P_n/g_s$ was observed at the highest leaf
408 temperature (47.9 ± 2.0°C) where $P_n/g_s$ was reduced by 35.8%. Thus, by inhibiting isoprenoid
409 biosynthesis, photosynthetic capacity is reduced at high temperatures in *V. guianensis.*

410 **4. Discussion**

411 Current mechanistic isoprene emission models predict that high temperatures are associated with
412 an enhanced rate of the production of the energetic and reductive equivalents necessary for
413 isoprenoid biosynthesis generated by the photochemical phase of photosynthesis. However, even
414 though tropical forests are the largest global source of isoprene in the atmosphere, whether the link
415 between high ETR and isoprene emission is valid in tropical trees had not been tested. We lacked
416 a quantitative assessment of the relationship between ETR and isoprene emissions in the tropics.

417 Using coupled gas exchange, chlorophyll fluorescence, and isoprene emission observations
418 during controlled leaf temperature response curves of *V. guianensis*, an early successional species
419 in the central Amazon, we provide evidence that temperature induced stimulation of isoprene
420 emissions is tightly correlated with ETR and $q_L$, both of which indicate a stimulation in the rate of
421 light-dependent NADPH and ATP production in the chloroplast (Niinemets *et al.*, 2002a,b). We
422 observed this strong temperature stimulation, and a near perfect coupling between isoprene

423 emissions and ETR and $q_L$, despite a decline in $g_s$ and $P_n$ at high temperatures. The high
424 temperatures did not alter the maximum photochemical efficiency of PSII as demonstrated by a
425 near constant Fv'/Fm' (supplementary data, **figure S1**) value of 0.57 over the range of the entire
426 leaf temperature measurement regime, nor were other photoprotective mechanisms, such as NPQ,
427 induced under these conditions. Assisted by solar heating of the leaf chamber during the Amazon
428 dry season, leaf temperatures during controlled temperature response curves reached values up to
429 50°C with isoprene emissions continuing to increase (see **Fig. 3**). Thus, rather than scaling down
430 the photochemical reactions of photosynthesis at high temperatures and increasing NPQ rates, the
431 photochemical reactions of *V. guianensis* leaves continue to increase likely through a tight
432 coupling to increased demand by non-$CO_2$ consuming metabolic pathways for photochemically
433 generated NADPH and/or ATP at high temperatures. This provides direct evidence that
434 suppression of $P_n$ at high leaf temperatures in the tropics is mainly associated with reductions in
435 $g_s$ rather than direct negative temperature effects on photosynthesis itself (Lloyd & Farquhar, 2008)
436 and is consistent with a previous study that observed a negative correlation between isoprene
437 emissions and NPQ (Pollastri *et al.*, 2014). Recently, isoprene photoprotection of photosynthesis
438 has been described through mechanisms alternative to NPQ, enabling plants to maintain a high
439 photosynthetic rates at rising temperatures by maintaining PSII and thylakoid membrane stability
440 (Pollastri *et al.*, 2019).

441 Notably, our results with *V. guianensis* stand in contrast to other studies including
442 field-grown cotton plants (a non-isoprene emitter) in North America, which regularly experience
443 temperatures of 40°C or higher during the growing season. It has been reported that components
444 of the photosynthetic apparatus in cotton leaves experience damage at high temperatures (35–
445 42°C) (Wise *et al.*, 2004). In a study carried out with the tropical tree *Inga edulis* in the central

446 Amazon (an isoprene emitter), it was observed that the rate of ETR declined after reaching 28-
447 36°C (Mendes *et al.*, 2017). Similar results were found in four species in a Malaysian rainforest,
448 where ETR declined after reaching a 35°C (Kitao *et al.*, 2000) and in a rainforest in Rwanda where
449 three species showed a decrease in ETR at leaf temperatures beyond 30°C and other three species
450 showed ETR declines above 35-37°C (Vårhammar *et al.*, 2015). As isoprene emissions were not
451 quantified in these studies, further studies are needed to determine if the continuous stimulation of
452 ETR and isoprene emissions to extreme leaf temperatures is a unique functional trait characteristic
453 of *V. guianensis*, or also a common occurrence in other early and late successional species in the
454 tropics that are regularly exposed to full sun and extreme daytime temperatures.

455 While the atmospheric roles of isoprene have been extensively investigated (Grosjean *et*
456 *al.*, 1993), much less is known about its biological roles including potential direct and indirect
457 impacts on the terrestrial carbon cycle during climate warming. Directly, leaf isoprene emissions
458 to the atmosphere represent a small (e.g. 5% at a leaf temperature of 50°C, **Fig. 3**), but potentially
459 important loss of carbon from tropical forests as surface temperatures increase (Harley *et al.*,
460 1996). In addition to this direct impact on the carbon cycle through a loss of ecosystem carbon,
461 our results are consistent with a secondary effect; isoprene production at high temperatures may
462 minimize the suppression in $P_n$ during high temperature extremes, and improve recovery rates
463 once more favorable temperatures are encountered (Sharkey *et al.*, 2001). This is supported by the
464 observations that blocking the isoprenoid pathway with fosmidomycin in *V. guianensis* repressed
465 $P_n$ at high temperatures through a mechanism that was independent of stomatal closure (**Figs. 3-**
466 **4**). Whether this is a consequence of the direct thermoprotective and signaling effects of isoprene
467 itself or other isoprenoid intermediates and products, or the loss of a major chloroplastic NADPH
468 and ATP consuming pathway at high temperatures will be a focus of future work. Although

469 fosmidomycin is considered highly specific and does not directly inhibit photosynthesis (Sharkey
470 *et al.*, 2001), it has been shown to rapidly (with 1 hour) reduce $P_n$, PSII chlorophyll fluorescence,
471 $V_{cmax}$ (the maximum rate of Ribulose-1,5-bisphosphate carboxylase activity) and $J_{max}$ (the
472 maximum rate of photosynthetic electron transport) (Possell *et al.*, 2010). Thus, care should be
473 taken in attributing these effects solely to a lack of isoprene as fosmidomycin negatively impacts
474 the synthesis of numerous other isoprenoids involved in photosynthesis resulting in
475 photoinhibition and photo-damage (Possell *et al.*, 2010). However, that the direct inhibition of
476 photosynthetic capacity with fosmidomycin in this experiment was only observed at
477 temperatures well in excess of the optimum $P_n$ temperature is consistent with the role of isoprene
478 in maintaining high photosynthetic capacity under thermal stress conditions in tropical species.
479 A recent literature survey of tropical plants reported that maximum temperatures for $P_n$ ~1.8°C
480 higher for isoprene-emitting species than for non-emitters, and thermal response curves were 24%
481 wider (Taylor *et al.*, 2019). Consistent with a significant impact on the ability of tropical forests to
482 maintain a strong carbon sink throughout the 21$^{st}$ century, this study suggested that isoprene
483 emission may be an adaptation to warmer thermal niches, and that emitting species may fare better
484 under global warming than co-occurring non-emitting species. However, the direct and indirect
485 impacts of isoprene emission on terrestrial carbon cycling in the tropics during high temperature
486 extremes remains to be quantified.

487 As isoprene emissions itself may represent a small fraction of ETR (Lantz *et al.*, 2019), we
488 estimated this fraction by using the slope of the linear relationship in **Eq. 7** (0.37 nmol
489 isoprene/μmol $e^-$). Thus, we estimate that as temperatures vary, the percentage of electrons leading
490 to isoprene biosynthesis is 0.037%. Thus, it is important to note that even at high temperatures,
491 only a small fraction of the reducing equivalents generated by ETR will be directly consumed for

492 isoprene biosynthesis and the strong coupling of ETR/$q_L$ and isoprene biosynthesis must be
493 supported by the induction of other pathways that consume the bulk of photosynthetically-derived
494 NADPH and ATP including the biosynthesis of non-volatile isoprenoids as well as other linked
495 biochemical processes and pathways such as photorespiration (Voss *et al.*, 2013), the re-
496 assimilation of respiratory and photorespiratory $CO_2$ (Garcia *et al*., 2019), the malate valve
497 (Rasulov *et al.*, 2018), mitochondrial respiration (Loreto *et al.*, 2007), and the alternate oxidase
498 pathway (Atkin & Tjoelker, 2003) (**Fig. 5**). For example, as leaf temperatures increase,
499 photorespiration rates rise faster than photosynthetic rates and an increasing proportion of the
500 NADPH and ATP are diverted into photorespiration (Long, 1991). Moreover, as temperatures
501 increase a large fraction of photorespiratory $CO_2$ can be re-assimilated by photosynthesis (Voss *et*
502 *al.*, 2013) and photorespiratory intermediates are increasingly incorporated into isoprene emissions
503 (Jardine *et al.*, 2014). Thus, despite isoprene emissions representing a small fraction of ETR (e.g.
504 0.037%), our observations are consistent with a mechanism where isoprenoid biosynthesis
505 operates in parallel with numerous coupled pathways which accelerate under high temperature to
506 create a positive feedback with ETR to maintain high photosynthetic capacity.

507 Previous research suggested that large variations in isoprene emissions as a function of
508 light, $CO_2$, temperature and oxygen were driven by the energy status of chloroplasts (Rasulov *et*
509 *al.*, 2009; Morfopoulos *et al.*, 2013); a result predicted by models of plant isoprene emissions based
510 on available NADPH and ATP (Morfopoulos *et al.*, 2013, 2014). These mechanisms have been
511 incorporated into Earth system models (Pacifico *et al.*, 2011; Harrison *et al.*, 2013) which predict
512 regional to global emission patterns of isoprene linked to photosynthesis. Therefore, the
513 quantitative relationship presented here between ETR and isoprene emissions from an abundant
514 Neotropical early successional species can be used in future modeling studies to improve the

accuracy of simulations predicting large increases in tropical isoprene emissions associated with increased forest dynamics and climate warming.

The optimal temperature range for $P_n$ has been cited as 30-31°C as typical for climax tree species in terra-firme tropical forests (Lloyd & Farquhar, 2008; Jardine *et al.*, 2017a; Slot & Winter, 2017). For example, in Panama reported optimum temperatures for $P_n$ ranged from 28.4°C to 31.9°C without a significant difference detected between trees and lianas and dry and wet sites. Thus, *V. guianensis* appears to show a higher optimum temperature for $P_n$ than previously reported for tropical species (32.6 ± 0.4°C). Moreover, isoprene emissions continued to increase through the highest temperatures obtainable by the leaf gas exchange system (wet season greater than or equal to 38.3 ± 0.4°C: **Figs. 1-2**, dry season 48.1 ± 2.0°C: **Fig. 3**). Thus, *V. guianensis* shows a dramatically higher optimum temperature for isoprene emissions than reported for other species (up to 10°C higher). To our knowledge, this represents the highest reported leaf temperature by which isoprene emissions continue to be stimulated by increasing temperature. These findings suggest that the photosynthetic apparatus in *V. guianensis,* and its coupling to isoprene production, is well adapted to the extreme high temperatures regularly experienced in secondary forests, in which the leaf temperature in the middle of the day and early afternoon regularly exceeds the ideal temperature range for $P_n$ (Doughty & Goulden, 2008), especially during the dry season and during droughts. For example, during the dry season of 2015-16 in a central Amazon rainforest, the upper canopy reached leaf temperatures > 45°C with strong afternoon suppression of $P_n$ associated with partial stomatal closure (Jardine et al., 2017a). A previous study with poplar leaves observed that the temperature optimum for $P_n$ (30°C) < ETR (35°C) < isoprene emissions (45°C) < enzyme activity of isoprene synthase (50°C) (Monson *et al.*, 1992). Thus, in order to determine the full extent of coupling of ETR and isoprene emission, future studies using engineered gas exchange

systems capable of extreme leaf temperatures (e.g. 25-60$^{o}$C) should be used to determine at what temperature ETR and isoprene emissions from *V. guianensis* finally begin to decline and if ETR and isoprene emissions share the same optimum leaf temperature.

As remote sensing of gross primary productivity using solar induced fluorescence (Yang *et al.*, 2015) and isoprene emissions (both direct isoprene observations and indirect via atmospheric formaldehyde columns measurements) (Zheng *et al.*, 2015; Fu *et al.*, 2019) are being evaluated from ecosystem to global scales, our mechanistic results may be utilized to better understand integrative studies on terrestrial carbon cycling in the tropics. For example, when atmospheric formaldehyde was used as a proxy for tropical isoprene emissions, it was found that isoprene emissions tracked the seasonal cycle of canopy temperature, but was anticorrelated with gross primary productivity (Foster *et al.*, 2014). In light of our leaf level observations, this could be explained by an increase in isoprene emissions and photochemical reactions of photosynthesis at high temperatures, but a suppression of $P_n$ associated with partial stomatal closure.

## 5. Acknowledgements

This material is based upon work supported as part of the Next Generation Ecosystem Experiments-Tropics (NGEE-Tropics) funded by the U.S. Department of Energy, Office of Science, Office of Biological and Environmental Research`s Terrestrial Ecosystem Science Program through contract No. DE-AC02-05CH11231 to Lawrence Berkeley National Laboratory, DE-AC05-00OR22725 to Oak Ridge National Laboratory, and DE-SC0012704 to Brookhaven National Laboratory. Additional funding for this research was provided by the Brazilian Conselho Nacional de Desenvolvimento Científico e Tecnológico (CNPq). Logistical and scientific support is acknowledged by the Forest Management laboratory (LMF), Climate and Environment

(CLIAMB), and Large Scale Biosphere-Atmosphere (LBA) programs at the National Institute for Amazon Research (INPA).

## 6. References

Affek HP, Yakir D (2003) Natural abundance carbon isotope composition of isoprene reflects incomplete coupling between isoprene synthesis and photosynthetic carbon flow. *Plant Physiology*, **131**, 1727–1736. DOI:10.1104/pp.102.012294

Alves EG, Harley P, Gonçalves JF de C, Moura CE da S, Jardine K (2014) Effects of light and temperature on isoprene emission at different leaf developmental stages of eschweilera coriacea in central Amazon. *Acta amazonica*, **44**, 9–18. DOI:10.1590/S0044-59672014000100002

Atkin OK, Tjoelker MG (2003) Thermal acclimation and the dynamic response of plant respiration to temperature. *Trends in Plant Science*, **8**, 343–351. DOI: 10.1016/S1360-1385(03)00136-5

Baker NR, Rosenqvist E (2004) Applications of chlorophyll fluorescence can improve crop production strategies: an examination of future possibilities. *Journal of Experimental Botany*, **55**, 1607–1621. DOI: 10.1093/jxb/erh196

Beer C, Reichstein M, Tomelleri E et al. (2010) Terrestrial gross carbon dioxide uptake: global distribution and covariation with climate. *Science*, **329**, 834–838. DOI: 10.1126/science.1184984

Brienen RJW, Phillips OL, Feldpausch TR et al. (2015) Long-term decline of the Amazon carbon sink. *Nature*, **519**, 344–348. DOI: 10.1038/nature14283

Chambers JQ, Silver WL (2004) Some aspects of ecophysiological and biogeochemical responses of tropical forests to atmospheric change. *Philosophical Transactions of the Royal Society of London. Series B, Biological Sciences*, **359**, 463–476. DOI: 10.1098/rstb.2003.1424

Chambers JQ, Robertson AL, Carneiro VMC, Lima AJN, Smith M-L, Plourde LC, Higuchi N (2009) Hyperspectral remote detection of niche partitioning among canopy trees driven by blowdown gap disturbances in the Central Amazon. *Oecologia*, **160**, 107–117. DOI: 10.1007/s00442-008-1274-9

Dani KGS, Jamie IM, Prentice IC, Atwell BJ (2015) Species-specific photorespiratory rate, drought tolerance and isoprene emission rate in plants. *Plant Signaling & Behavior*, **10**, e990830. DOI: 10.4161/15592324.2014.990830

Delwiche CF, Sharkey TD (1993) Rapid appearance of 13C in biogenic isoprene when 13CO2 is fed to intact leaves. *Plant, Cell & Environment*, **16**, 587–591. DOI: 10.1111/j.1365-3040.1993.tb00907.x

Doughty CE, Goulden ML (2008) Are tropical forests near a high temperature threshold? *Journal of Geophysical Research: Biogeosciences*, **113**. DOI:10.1029/2007JG000632

Duncan BN, Yoshida Y, Damon MR, Douglass AR, Witte JC (2009) Temperature dependence of factors controlling isoprene emissions. *Geophysical Research Letters*, **36**. DOI: 10.1029/2008GL037090

Earl HJ, Tollenaar M (1998) Relationship between thylakoid electron transport and photosynthetic CO2 uptake in leaves of three maize (Zea mays L.) hybrids. *Photosynthesis Research*. DOI: 10.1023/A:1006198821912

Foster PN, Prentice IC, Morfopoulos C (2014) Isoprene emissions track the seasonal cycle of canopy temperature, not primary production: evidence from remote sensing. *Biogeosciences*, **11**, 3437–3451. DOI:10.5194/bg-11-3437-2014

Funk JL, Mak JE, Lerdau MT (2004) Stress-induced changes in carbon sources for isoprene production in Populus deltoides. *Plant, Cell & Environment*, **27**, 747–755. DOI: 10.1111/j.1365-3040.2004.01177.x

Fu D, Millet DB, Wells KC, Payne VH, Yu S, Guenther A, Eldering A (2019) Direct retrieval of isoprene from satellite-based infrared measurements. *Nature Communications*, **10**, 3811. DOI: 10.1038/s41467-019-11835

Garcia S, Jardine K, Souza V, Souza R, Duvoisin Junior S, Gonçalves J (2019) Reassimilation of Leaf Internal CO2 Contributes to Isoprene Emission in the Neotropical Species *Inga edulis* Mart. *Forests*, **10**, 472. DOI: 10.3390/f10060472

Goulden ML, Miller SD, da Rocha HR, Menton MC, de Freitas HC, e Silva Figueira AM, de Sousa CAD (2004) Diel and seasonal patterns of tropical forest $CO_2$ exchange. Ecological Applications, **14**, 42–54. DOI: 10.1890/02-6008

Grosjean D, Williams EL, Grosjean E (1993) Atmospheric chemistry of isoprene and of its carbonyl products. *Environmental science & technology*, **27**, 830–840. DOI: 10.1021/es00042a004

Guenther A, Karl T, Harley P, Wiedinmyer C, Palmer PI, Geron C (2006) Estimates of global terrestrial isoprene emissions using MEGAN (Model of Emissions of Gases and Aerosols from Nature). *Atmospheric Chemistry and Physics*, **6**, 3181–3210. DOI: 10.5194/acp-6-3181-2006

Guidolotti G, Pallozzi E, Gavrichkova O, Scartazza A, Mattioni M, Loreto F, Calfapietra C (2019) Emission of constitutive isoprene, induced monoterpenes, and other volatiles under hight temperatures in *Eucalyptus camaldulensis*: A $^{13}C$ labelling study. *Plant, Cell & Environment*, **42**, 1929-1938. DOI: 10.1111/pce.13521

Harley P, Guenther A, Zimmerman P (1996) Effects of light, temperature and canopy position on net photosynthesis and isoprene emission from sweetgum (Liquidambar styraciflua) leaves. *Tree Physiology*, **16**, 25–32. DOI: 10.1093/treephys/16.1-2.25

Harley PC, Monson RK, Lerdau MT (1999) Ecological and evolutionary aspects of isoprene emission from plants. *Oecologia*, **118**, 109–123. DOI: 10.1007/s004420050709

Harrison SP, Morfopoulos C, Dani KGS et al. (2013) Volatile isoprenoid emissions from plastid to planet. *The New Phytologist*, **197**, 49–57. DOI: 10.1111/nph.12021

Higuchi N, dos Santos J, Vieira G et al. (1998) Análise estrutural da floresta primária da bacia do rio Cuieiras, ZF-2, Manaus-AM, Brasil. *Acta Amazonica*, **28**, 153–166.

Himalayan O, Tech B (2005) Physiological basis of seasonal trend in leaf photosynthesis of five evergreen broad-leaved species in a temperate deciduous forest. *Tree Physiology*, **4**, 249–256. DOI: 10.1093/treephys/26.2.249

Ishida A, Toma T (1999) Limitation of leaf carbon gain by stomatal and photochemical processes in the top canopy of. *Tree Physiology*. DOI: 10.1093/treephys/19.7.467

Jardine KJ, Sommer ED, Saleska SR, Huxman TE, Harley PC, Abrell L (2010) Gas phase measurements of pyruvic acid and its volatile metabolites. *Environmental science & technology*, **44**, 2454–2460. DOI: 10.1021/es903544p

Jardine K, Yañez Serrano A, Arneth A et al. (2011) Within-canopy sesquiterpene ozonolysis in Amazonia. *Journal of Geophysical Research*, **116**. DOI: 10.1029/2011JD016243

Jardine KJ, Monson RK, Abrell L et al. (2012) Within-plant isoprene oxidation confirmed by direct emissions of oxidation products methyl vinyl ketone and methacrolein. *Glob Change Biol*, **18**, 973–984. DOI: 10.1111/j.1365-2486.2011.02610.x

Jardine K, Chambers J, Alves EG et al. (2014) Dynamic balancing of isoprene carbon sources reflects photosynthetic and photorespiratory responses to temperature stress. *Plant Physiology*, **166**, 2051–2064. DOI: https://doi.org/10.1104/pp.114.247494

Jardine AB, Jardine KJ, Fuentes JD et al. (2015a) Highly reactive light-dependent monoterpenes in the Amazon. *Geophysical Research Letters*, **42**, 1576–1583. DOI: 10.1002/2014GL062573

Jardine KJ, Chambers JQ, Holm J et al. (2015b) Green Leaf Volatile Emissions during High Temperature and Drought Stress in a Central Amazon Rainforest. *Plants*, **4**, 678–690. DOI: 10.3390/plants4030678

Jardine KJ, Jardine AB, Souza VF et al. (2016) Methanol and isoprene emissions from the fast growing tropical pioneer species *Vismia guianensis* (Aubl.) Pers. (Hypericaceae) in the central Amazon forest. *Atmospheric Chemistry and Physics*, **16**, 6441–6452. DOI: 10.5194/acp-16-6441-2016

Jardine KJ, Jardine AB, Holm JA et al. (2017a) Monoterpene "thermometer" of tropical forest-atmosphere response to climate warming. *Plant, Cell & Environment*, **40**, 441–452. DOI: 10.1104/pp.102.012294

Jardine KJ, Fernandes de Souza V, Oikawa P et al. (2017b) Integration of $C_1$ and $C_2$ metabolism in trees. *International Journal of Molecular Sciences*, **18**. DOI: 10.3390/ijms18102045

[dataset] Jardine K; Rodrigues T (2019): Isoprene, Chlorophyll fluorescence, and leaf temperature data from Manaus, Brazil, 2017 - 2018. 1.0. NGEE Tropics Data Collection. (dataset). http://dx.doi.org/10.15486/ngt/1570407

Karl T, Guenther A, Turnipseed A, Tyndall G, Artaxo P, Martin S (2009) Rapid formation of isoprene photo-oxidation products observed in Amazonia. *Atmospheric Chemistry and Physics*, **9**, 7753–7767. DOI: 10.5194/acp-9-7753-2009

Karl T, Harley P, Emmons L et al. (2010) Efficient atmospheric cleansing of oxidized organic trace gases by vegetation. *Science*, **330**, 816–819. DOI: 10.1126/science.1192534

Kitao M, Lei TT, Koike T, Tobita H, Maruyama Y, Matsumoto Y, Ang L-H (2000) Temperature response and photoinhibition investigated by chlorophyll fluorescence measurements for four distinct species of dipterocarp trees. *Physiologia Plantarum*, **109**, 284–290. DOI: 10.1034/j.1399-3054.2000.100309.x

Koch GW, Amthor JS., Goulden ML (1994) Diurnal patterns of leaf photosynthesis, conductance and water potential at the top fo a lowland rain forest canopy in cameroon: measurements from the Radeau des Cimes. *Tree Physiology*, **14**, 347–360. DOI: 10.1093/treephys/14.4.347

Koren G, van Schaik E, Araújo AC et al. (2018) Widespread reduction in sun-induced fluorescence from the Amazon during the 2015/2016 El Niño. *Philosophical Transactions of the Royal Society of London. Series B, Biological Sciences*, **373**. DOI: 10.1098/rstb.2017.0408

Kramer DM, Johnson G (2004) Kiirats 0, et al. New Fluorescence Parame-ters for the Determination of QA Redox State and Excitation EnergyFluxes. *Photosynthesis Research*, **79**, 209–218. DOI: 10.1023/B:PRES.0000015391.99477.0d

Krause GH, Weis E (1984) Chlorophyll fluorescence as a tool in plant physiology: II. Interpretation of fluorescence signals. *Photosynthesis Research*, **5**, 139–157. DOI: 10.1007/BF00028527

Kreuzwieser J, Graus M, Wisthaler A, Hansel A, Rennenberg H, Schnitzler J-P (2002) Xylem-transported glucose as an additional carbon source for leaf isoprene formation in Quercus robur. *The New Phytologist*, **156**, 171–178. DOI: 10.1046/j.1469-8137.2002.00516.x

Lantz AT, Allman J, Weraduwage SM, Sharkey TD (2019) Isoprene: New insights into the control of emission and mediation of stress tolerance by gene expression. *Plant, Cell & Environment*, **42**, 2808–2826. DOI: 10.1111/pce.13629

Lichtenthaler HK (1999) The 1-Deoxy-D-Xylulose-5-Phosphate Pathway of Isoprenoid Biosynthesis in Plants. *Annual review of plant physiology and plant molecular biology*, **50**, 47–65. DOI: 10.1146/annurev.arplant.50.1.47

Liu J, Bowman KW, Schimel DS et al. (2017) Contrasting carbon cycle responses of the tropical continents to the 2015-2016 El Niño. *Science*, **358**. DOI: 10.1126/science.aam5690

Li Z, Wakao S, Fischer BB, Niyogi KK (2009) Sensing and responding to excess light. *Annual review of plant biology*, **60**, 239–260. DOI: 10.1146/annurev.arplant.58.032806.103844

Li Z, Ratliff EA, Sharkey TD (2011) Effect of temperature on postillumination isoprene emission in oak and poplar. *Plant Physiology*, **155**, 1037–1046. DOI: 10.1104/pp.110.167551

Lloyd J, Farquhar GD (2008) Effects of rising temperatures and [CO2] on the physiology of tropical forest trees. *Philosophical Transactions of the Royal Society of London. Series B, Biological Sciences*, **363**, 1811–1817. DOI: 10.1098/rstb.2007.0032

Long SP (1991) Modification of the response of photosynthetic productivity to rising temperature by atmospheric $CO_2$ concentrations: Has its importance been underestimated? *Plant, Cell & Environment*, **14**, 729–739. DOI: 10.1111/j.1365-3040.1991.tb01439.x

Loreto F, Sharkey TD (1990) A gas-exchange study of photosynthesis and isoprene emission inQuercus rubra L. *Planta*, **182**, 523–531. DOI: 10.1007/BF02341027

Loreto F, Centritto M, Barta C, Calfapietra C, Fares S, Monson RK (2007) The relationship between isoprene emission rate and dark respiration rate in white poplar (*Populus alba* L.) leaves. *Plant, Cell & Environment*, **30**, 662–669. DOI: 10.1111/j.1365-3040.2007.01648.x

Mendes KR, Marenco RA, Nascimento HCS (2017) Maximum carboxylation velocity of RUBISCO and maximum rate of electron transport in saplings in response to variations in environmental factors in central Amazonia. *Ciência Florestal*, **27**, 947–959.

Mesquita RCG, Delamônica P, Laurance WF (1999) Effect of surrounding vegetation on edge-related tree mortality in Amazonian forest fragments. *Biological Conservation*, **91**, 129–134. DOI: 10.1016/S0006-3207(99)00086-5

Mesquita R de CG, Massoca PE dos S, Jakovac CC, Bentos TV, Williamson GB (2015) Amazon Rain Forest Succession: Stochasticity or Land-Use Legacy? *Bioscience*, **65**, 849–861. DOI: 10.1093/biosci/biv108

Mittler R (2017) ROS Are Good. *Trends in Plant Science*, **22**, 11–19. DOI: 10.1016/j.tplants.2016.08.002

Monson RK, Jaeger CH, Adams WW, Driggers EM, Silver GM, Fall R (1992) Relationships among Isoprene Emission Rate, Photosynthesis, and Isoprene Synthase Activity as Influenced by Temperature. *Plant Physiology*, **98**, 1175–1180. DOI: 10.1104/pp.98.3.1175

Morfopoulos C, Prentice IC, Keenan TF, Friedlingstein P, Medlyn BE, Peñuelas J, Possell M (2013) A unifying conceptual model for the environmental responses of isoprene emissions from plants. *Annals of Botany*, **112**, 1223–1238. DOI: 10.1093/aob/mct206

Morfopoulos C, Sperlich D, Peñuelas J et al. (2014) A model of plant isoprene emission based on available reducing power captures responses to atmospheric $CO_2$. *New Phytologist*, **203**, 125–139. DOI: 10.1111/nph.12770

Müller P, Li XP, Niyogi KK (2001) Non-photochemical quenching. A response to excess light energy. *Plant Physiology*, **125**, 1558–1566. DOI: 10.1104/pp.125.4.1558

Murchie EH, Lawson T (2013) Chlorophyll fluorescence analysis: a guide to good practice and understanding some new applications. *Journal of Experimental Botany*, **64**, 3983–3998. DOI: 10.1093/jxb/ert208

Niinemets U, Hauff K, Bertin N, Tenhunen JD, Steinbrecher R, Seufert G (2002a) Monoterpene emissions in relation to foliar photosynthetic and structural variables in Mediterranean evergreen Quercus species. *The New Phytologist*, **153**, 243–256. DOI: 10.1046/j.0028-646X.2001.00323.x

Niinemets U, Seufert G, Steinbrecher R, Tenhunen JD (2002b) A model coupling foliar monoterpene emissions to leaf photosynthetic characteristics in Mediterranean evergreen Quercus species. *The New Phytologist*, **153**, 257–275. DOI: 10.1046/j.0028-646X.2001.00324.x

Pacifico F, Harrison SP, Jones CD, Sitch S (2009) Isoprene emissions and climate. *Atmospheric environment*, **43**, 6121–6135. DOI: 10.1016/j.atmosenv.2009.09.002

759 Pacifico F, Harrison SP, Fu TM et al. (2011) Evaluation of a photosynthesis-based biogenic
760 isoprene emission scheme in JULES and simulation of isoprene emissions under present-
761 day climate conditions. DOI:10.5194/acp-11-4371-2011
762 Piedade MTF, Long SP, Junk WJ (1994) Leaf and canopy photosynthetic $CO_2$ uptake of a stand
763 of Echinochloa polystachya on the Central Amazon floodplain: Are the high potential rates
764 associated with the C4 syndrome realized under the near-optimal conditions provided by
765 this exceptional natural habitat? *Oecologia*, **97**, 193–201. DOI: 10.1007/BF00323149
766 Pollastri S, Tsonev T, Loreto F (2014) Isoprene improves photochemical efficiency and
767 enhances heat dissipation in plants at physiological temperatures. *Journal of Experimental*
768 *Botany*, **65**, 1565–1570. DOI: 10.1093/jxb/eru033
769 Pollastri S, Jorba I, Hawkins TJ et al. (2019) Leaves of isoprene-emitting tobacco plants
770 maintain PSII stability at high temperatures. *The New Phytologist*, **223**, 1307–1318. DOI:
771 10.1111/nph.15847
772 Possell M, Ryan A, Vickers CE, Mullineaux PM, Hewitt CN (2010) Effects of fosmidomycin on
773 plant photosynthesis as measured by gas exchange and chlorophyll fluorescence.
774 *Photosynthesis Research*, **104**, 49–59. DOI: 10.1007/s11120-009-9504-5
775 Potter C, Klooster S, Hiatt C, Genovese V, Castilla-Rubio JC (2011) Changes in the carbon
776 cycle of Amazon ecosystems during the 2010 drought. *Environmental Research Letters*, **6**,
777 034024. DOI:10.1088/1748-9326/6/3/034024
778 Rapparini F, Baraldi R, Miglietta F, Loreto F (2004) Isoprenoid emission in trees of Quercus
779 pubescens and Quercus ilex with lifetime exposure to naturally high $CO_2$ environment+.
780 *Plant, Cell & Environment*, **27**, 381–391. DOI: 10.1111/j.1365-3040.2003.01151.x
781 Rasulov B, Hüve K, Välbe M, Laisk A, Niinemets U (2009) Evidence that light, carbon dioxide,
782 and oxygen dependencies of leaf isoprene emission are driven by energy status in hybrid
783 aspen. *Plant Physiology*, **151**, 448–460. DOI: 10.1104/pp.109.141978
784 Rasulov B, Talts E, Bichele I, Niinemets Ü (2018) Evidence that isoprene emission is not limited
785 by cytosolic metabolites. exogenous malate does not invert the reverse sensitivity of
786 isoprene emission to high [$CO_2$]. *Plant Physiology*, **176**, 1573–1586. DOI:
787 10.1104/pp.17.01463
788 Sage RF, Kubien DS (2007) The temperature response of C(3) and C(4) photosynthesis. *Plant,*
789 *Cell & Environment*, **30**, 1086–1106. DOI: 10.1111/j.1365-3040.2007.01682.x
790 Sanadze GA (1991) Isoprene Effect—Light-Dependent Emission of Isoprene by Green Parts of
791 Plants. In: *Trace gas emissions by plants*, pp. 135–152. Elsevier.
792 Sasaki K, Saito T, Lämsä M et al. (2007) Plants utilize isoprene emission as a thermotolerance
793 mechanism. *Plant & Cell Physiology*, **48**, 1254–1262. DOI: 10.1093/pcp/pcm104
794 Sharkey TD (2005) Effects of moderate heat stress on photosynthesis: importance of thylakoid
795 reactions, rubisco deactivation, reactive oxygen species, and thermotolerance provided by
796 isoprene. *Plant, Cell & Environment*, **28**, 269–277. DOI: 10.1111/j.1365-3040.2005.01324.x
797 Sharkey TD, Yeh S (2001) Isoprene emission from plants. *Annual Review of Plant Physiology*
798 *and Plant Molecular Biology*, **52**, 407–436. DOI: 10.1146/annurev.arplant.52.1.407
799 Sharkey TD, Chen X, Yeh S (2001) Isoprene increases thermotolerance of fosmidomycin-fed
800 leaves. *Plant Physiology*, **125**, 2001–2006. DOI: 10.1104/pp.125.4.2001
801 Silver GM, Fall R (1995) Characterization of aspen isoprene synthase, an enzyme responsible
802 for leaf isoprene emission to the atmosphere. *The Journal of Biological Chemistry*, **270**,
803 13010–13016. DOI: 10.1074/jbc.270.22.13010
804 Singsaas EL, Lerdau M, Winter K, Sharkey TD (1997) Isoprene Increases Thermotolerance of
805 Isoprene-Emitting Species. *Plant Physiology*, **115**, 1413–1420. DOI:
806 10.1104/pp.115.4.1413
807 Slot M, Winter K (2017) In situ temperature response of photosynthesis of 42 tree and liana
808 species in the canopy of two Panamanian lowland tropical forests with contrasting rainfall
809 regimes. *The New Phytologist*, **214**, 1103–1117. DOI: 10.1111/nph.14469

de Souza VF, Niinemets Ü, Rasulov B, Vickers CE, Duvoisin Júnior S, Araújo WL, Gonçalves JF de C (2018) Alternative carbon sources for isoprene emission. *Trends in Plant Science*, **23**, 1081–1101. DOI: 10.1016/j.tplants.2018.09.012

Stutz SS, Hanson DT (2019) Contribution and consequences of xylem-transported CO2 assimilation for C3 plants. *The New Phytologist*, **223**, 1230–1240. DOI: 10.1111/nph.15907

Taylor TC, Smith MN, Slot M, Feeley KJ (2019) The capacity to emit isoprene differentiates the photosynthetic temperature responses of tropical plant species. *Plant, Cell & Environment*, **42**, 2448–2457. DOI: 10.1111/pce.13564

Uhl C, Buschbacher R, Serrao EAS (1988) Abandoned pastures in eastern Amazonia. I. patterns of plant succession. *The Journal of Ecology*, **76**, 663. DOI: 10.2307/2260566

Vårhammar A, Wallin G, McLean CM et al. (2015) Photosynthetic temperature responses of tree species in Rwanda: evidence of pronounced negative effects of high temperature in montane rainforest climax species. *The New Phytologist*, **206**, 1000–1012. DOI: 10.1111/nph.13291

Velikova V, Fares S, Loreto F (2008) Isoprene and nitric oxide reduce damages in leaves exposed to oxidative stress. *Plant, Cell & Environment*, **31**, 1882–1894. DOI: 10.1111/j.1365-3040.2008.01893.x

Vickers CE, Gershenzon J, Lerdau MT, Loreto F (2009a) A unified mechanism of action for volatile isoprenoids in plant abiotic stress. *Nature Chemical Biology*, **5**, 283–291. DOI: 10.1038/nchembio.158

Vickers CE, Possell M, Cojocariu CI et al. (2009b) Isoprene synthesis protects transgenic tobacco plants from oxidative stress. *Plant, Cell & Environment*, **32**, 520–531. DOI: 10.1111/j.1365-3040.2009.01946.x

Voss I, Sunil B, Scheibe R, Raghavendra AS (2013) Emerging concept for the role of photorespiration as an important part of abiotic stress response. *Plant Biology*, **15**, 713–722. DOI: 10.1111/j.1438-8677.2012.00710.x

Wise RR, Olson AJ, Schrader SM, Sharkey TD (2004) Electron transport is the functional limitation of photosynthesis in field-grown Pima cotton plants at high temperature. *Plant, Cell & Environment*, **27**, 717–724. DOI: 10.1111/j.1365-3040.2004.01171.x

Yang X, Tang J, Mustard JF et al. (2015) Solar-induced chlorophyll fluorescence that correlates with canopy photosynthesis on diurnal and seasonal scales in a temperate deciduous forest. *Geophysical Research Letters*, **42**, 2977–2987. DOI: 10.1002/2015GL063201

Zalamea M, González G (2008) Leaf fall phenology in a subtropical wet forest in Puerto Rico: from species to community patterns. *Biotropica*, **40**, 295–304. DOI: 10.1111/j.1744-7429.2007.00389.x

Zheng Y, Unger N, Barkley MP, Yue X (2015) Relationships between photosynthesis and formaldehyde as a probe of isoprene emission. *Atmospheric Chemistry and Physics*, **15**, 8559–8576. DOI:10.5194/acp-15-8559-2015

Zuo Z, Weraduwage SM, Lantz AT et al. (2019) Isoprene acts as a signaling molecule in gene networks important for stress responses and plant growth. *Plant Physiology*, **180**, 124–152. DOI: 10.1104/pp.18.01391

## 7. Supplementary Material

Supplementary Figure S1 showing mean *V. guianensis* leaf temperature responses of fluorescence parameters including maximum quantum efficiency of PSII photochemistry in the light (Fv`/Fm`) and in the dark (Fv/Fm) is available for download as 'FigureS1_SuppInfo.pdf'.

## 8. Data Availability Statement

The data that support the findings of this study are openly available in NGEE Tropics Data Collection at http://dx.doi.org/10.15486/ngt/1570407, reference number BR-Ma2. The supplementary data (Size: 11,657 KB) includes raw data obtained from the Licor 6400XT gas exchange system and the TD-GC-MS system for isoprene emission analysis and organized as follows:

**Fluorescence experiment folder:**

- Gas exchange data (Licor 6400XT files) including fluorescence with leaf number and date
- Isoprene data (TD-GC-MS output files) with leaf number and date

**Inhibitor experiment folder:**

- Gas exchange data (Licor 6400XT files) and isoprene data (TD-GC-MS output files) with isoprenoid fed inhibitor: Folders separated by date
- Gas exchange data (Licor 6400XT files) and isoprene data (TD-GC-MS files) with water fed control branches: Folders separated by date

874 **9. Figures and Tables**

875

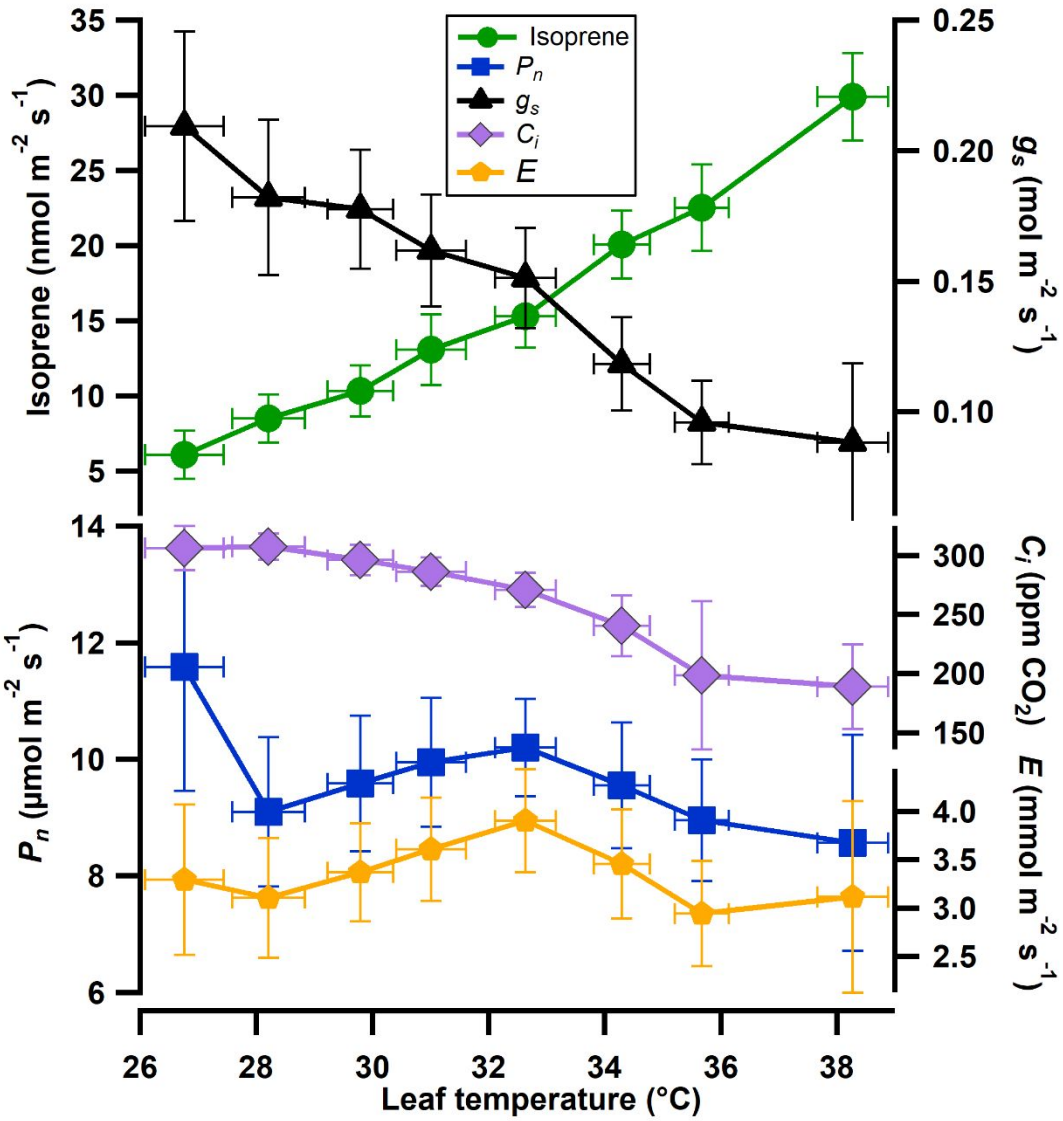


876

877 **Figure 1:** Mean response of net photosynthesis ($P_n$), stomatal conductance ($g_s$), internal carbon
878 ($C_i$), transpiration (E), and isoprene emissions to an increase in leaf temperature in *V. guianensis*.
879 Data shown are the mean of 23 temperature response curves collected with error bars representing
880 ± 2 standard deviation.

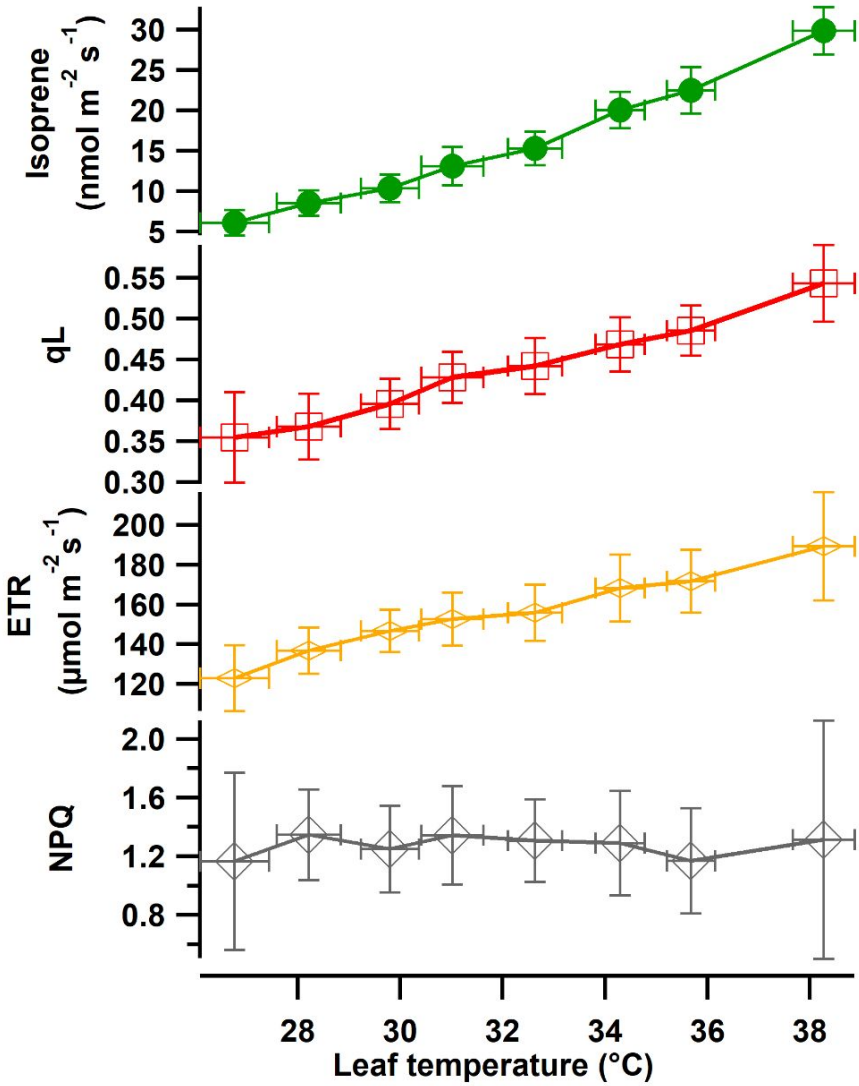


881

882 **Figure 2**: Mean *V. guianensis* leaf temperature responses of light-dependent photosynthetic
883 parameters including electron transfer rate (ETR), oxidation state of $Q_A$ ($q_L$), and non-
884 photochemical quenching (NPQ) together with leaf isoprene emissions. Data shown are the mean
885 of 23 temperature response curves collected with error bars representing ± 2 standard deviation.

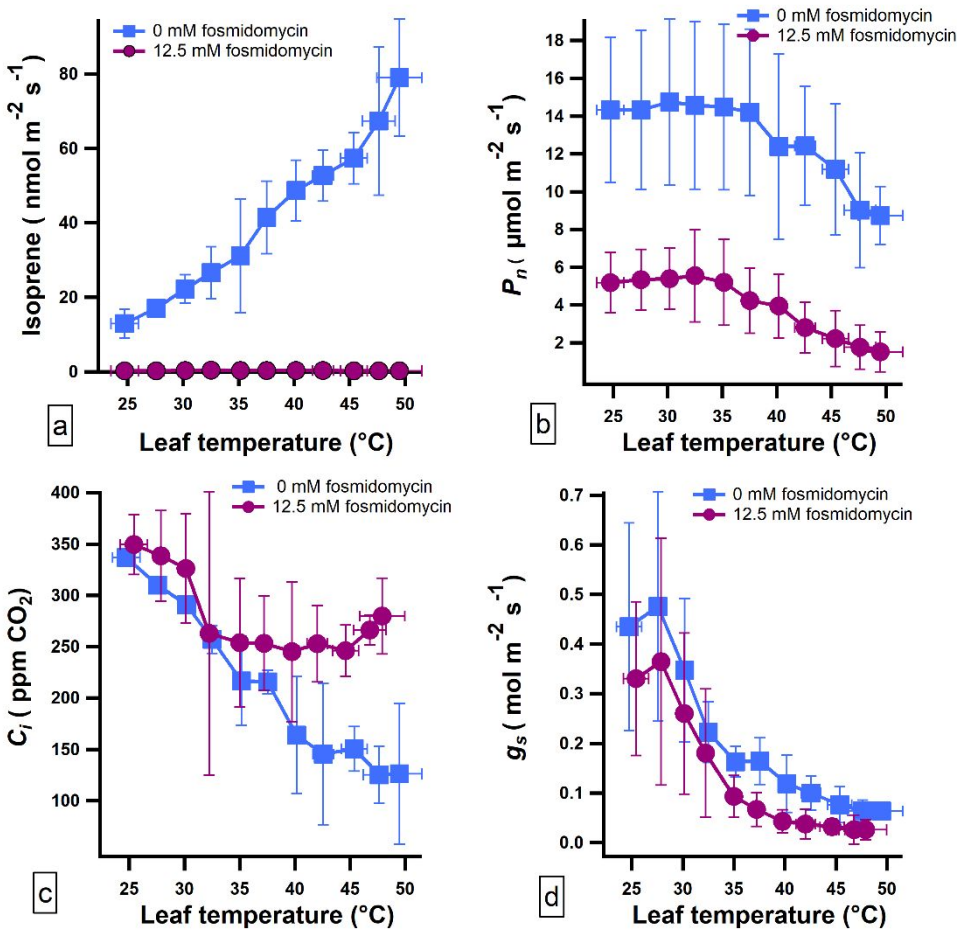


886
887 **Figure 3**: Mean *V. guianensis* leaf temperature responses after 1 hour of branch feeding with 0
888 mM (blue curves with squares) and 12.5 mM (purple curves with dots) of the isoprenoid pathway
889 inhibitor fosmidomycin showing (**a**) isoprene emissions, (**b**) net photosynthesis, $P_n$, (**c**)
890 intercellular $CO_2$ concentration, $C_i$, (**d**) stomatal conductance, $g_s$. Data shown are the mean of 3-4
891 temperature response curves (1 curve per leaf) with error bars representing ± 2 standard deviation.
892

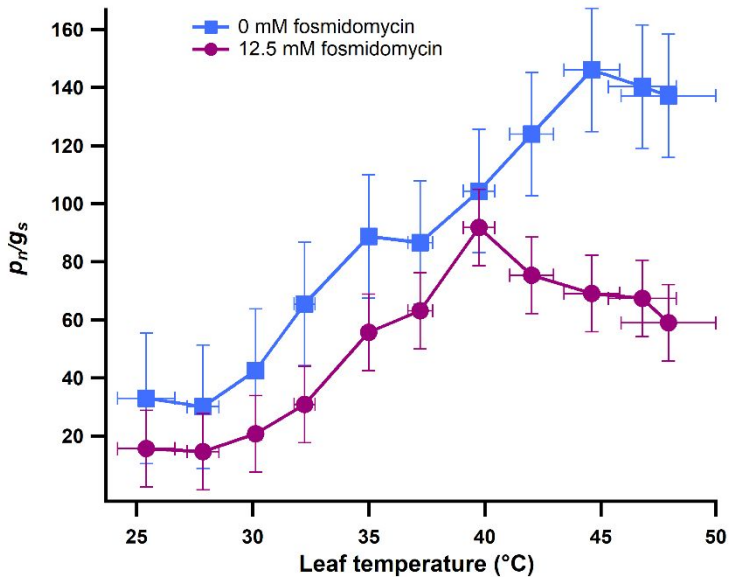


**Figure 4:** Mean *V. guianensis* leaf temperature responses after 1 hour of branch feeding with 0 mM (blue curves with squares) and 12.5 mM (purple curves with dots) of the isoprenoid pathway inhibitor fosmidomycin showing net photosynthesis normalized to stomatal conductance, $P_n/g_s$. Data shown are the mean of 3-4 temperature response curves (1 curve per leaf) with error bars representing ± 2 standard deviation.

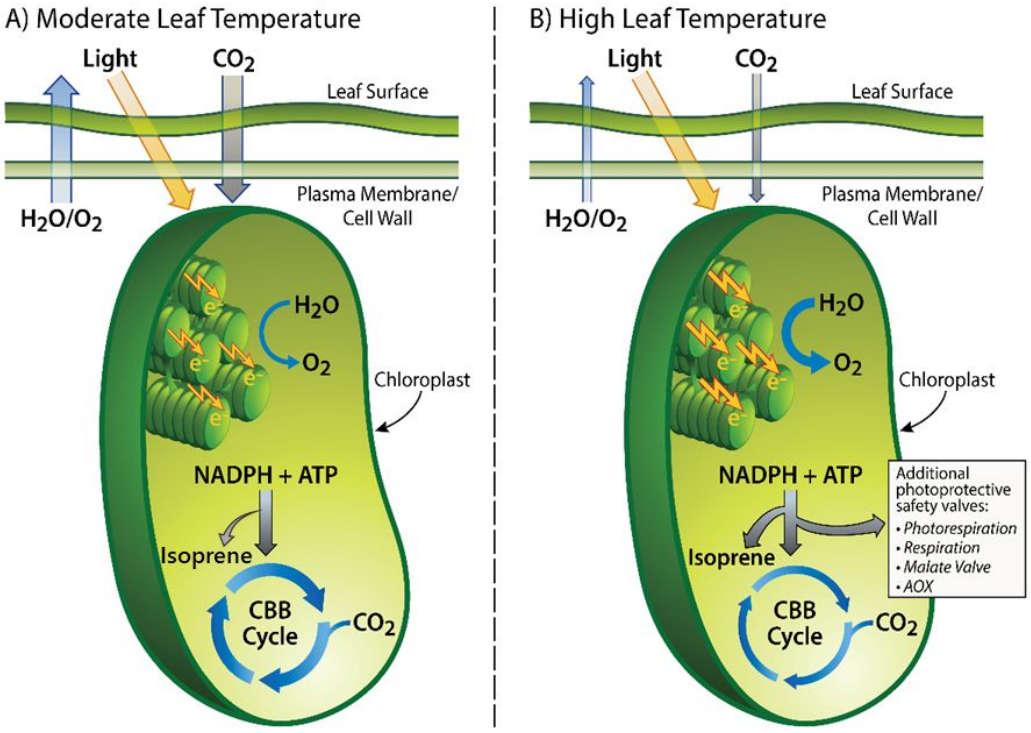

**Figure 5**: Proposed biochemical model of the acclimation to high temperature stress through the consumption of photosynthetic energy (ATP) and reducing equivalents (NADPH) through the activation of the isoprenoid pathway together in parallel with other coupled biochemical pathways (adapted from Voss *et al*., 2013 and Morfopoulos *et al*., 2014). $O_2$: oxygen; $CO_2$: carbon dioxide; $H_2O$: water; ATP: adenosine triphosphate; NADPH: Nicotinamide-Adenine-Dinucleotide-Phosphate; AOX: alternative oxidases of mitochondria.

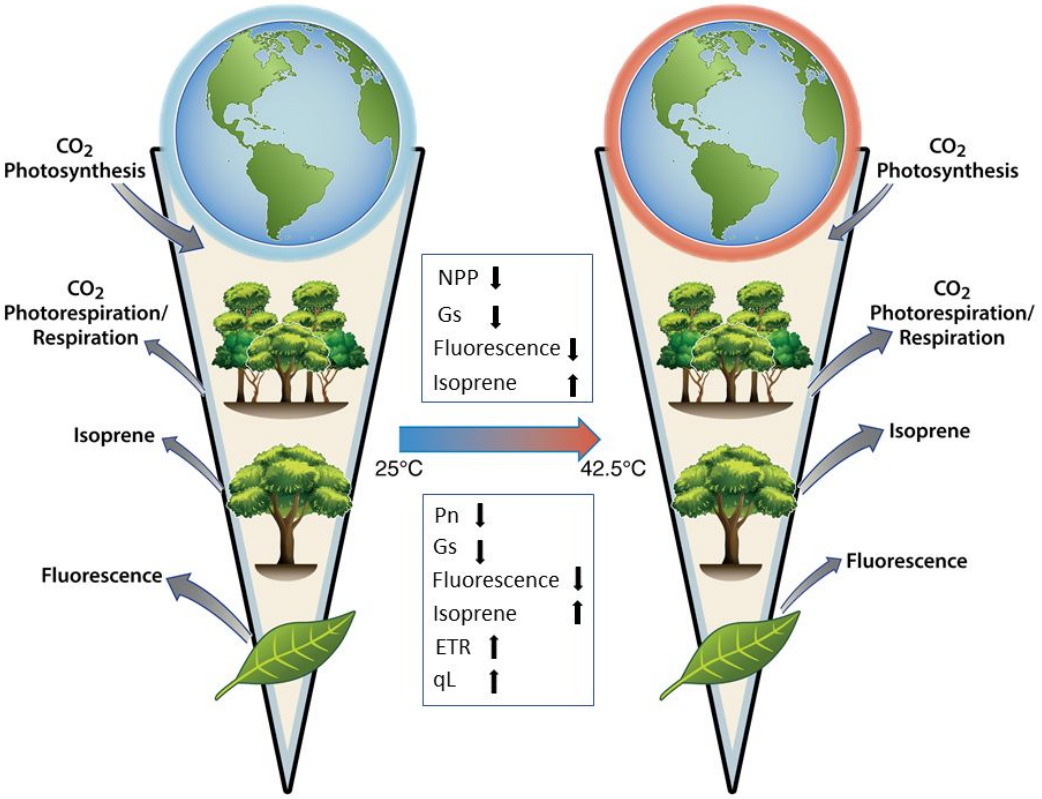


**Figure 6 (Graphical Abstract)**: Graphical representation the influence of proposed surface temperature impacts on plant physiological processes influencing terrestrial ecosystem carbon cycling from leaf to global scales. NPP: Net Primary Productivity, Gs: Stomatal Conductance, ETR: Electron Transport Rate, qL: Fraction of PSII centers that are oxidized, $CO_2$: carbon dioxide.

| | $P_n$ | $g_s$ | Fv'/Fm' | NPQ | ETR | Isoprene | $C_i$ | qL |
|---|---|---|---|---|---|---|---|---|
| ***$P_n$*** | 1 | 0.73 | 0.57 | -0.38 | -0.75 | -0.68 | 0.63 | -0.65 |
| ***$g_s$*** | 0.73 | 1 | 0.62 | -0.05 | -0.97 | -0.97 | 0.97 | -0.97 |
| ***Fv'/Fm'*** | 0.57 | 0.62 | 1 | -0.33 | -0.67 | -0.53 | 0.46 | -0.60 |
| ***NPQ*** | -0.38 | -0.05 | -0.33 | 1 | 0.19 | 0.09 | 0.13 | 0.13 |
| ***ETR*** | -0.75 | -0.97 | -0.67 | 0.19 | 1 | 0.98 | -0.93 | 0.99 |
| ***Isoprene*** | -0.69 | -0.97 | -0.53 | 0.09 | 0.98 | 1 | -0.97 | 0.99 |
| ***$C_i$*** | 0.63 | 0.97 | 0.46 | 0.13 | -0.93 | -0.97 | 1 | -0.95 |
| ***qL*** | -0.65 | -0.97 | -0.60 | 0.13 | 0.99 | 0.99 | -0.95 | 1 |

**Table 1**: Correlation ($r$) derived between the gas exchange ($P_n$, $g_s$, and isoprene emissions) and light-independent photosynthetic variables shown in **Figs. 1-2**.

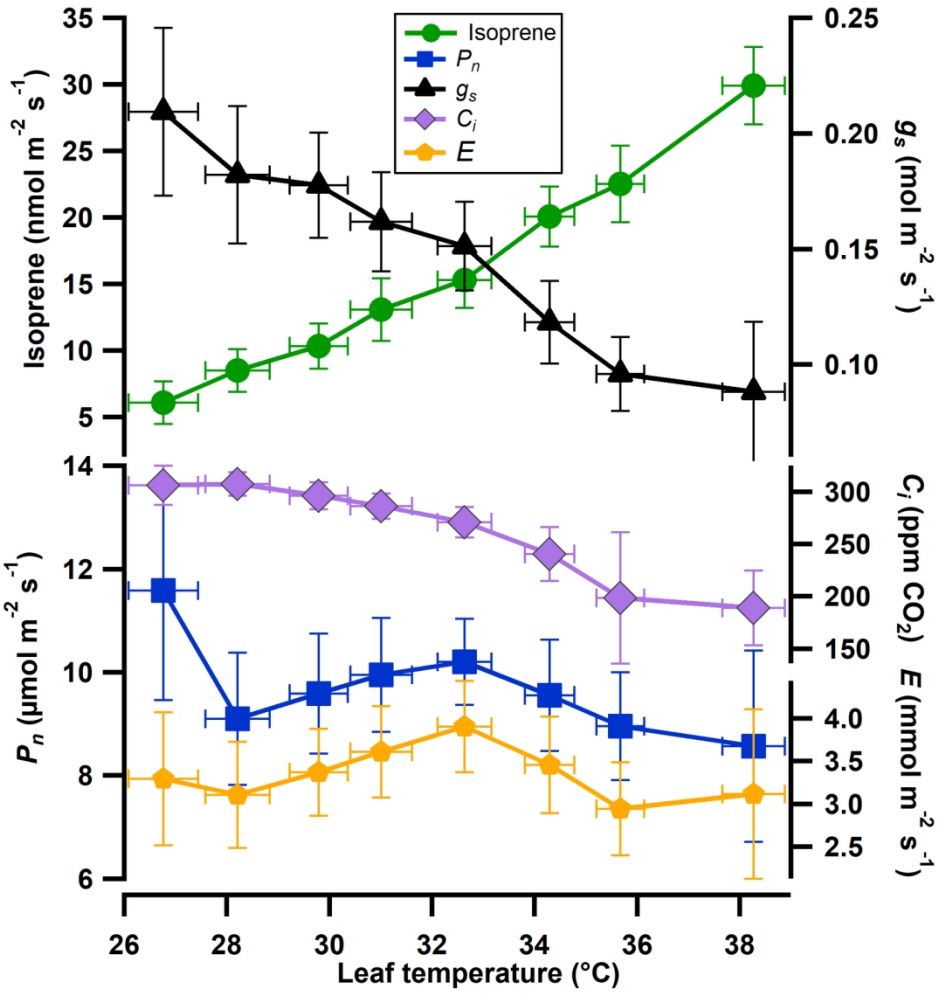


Figure 1: Mean response of net photosynthesis (Pn), stomatal conductance (gs), internal carbon (Ci), transpiration (E), and isoprene emissions to an increase in leaf temperature in V. guianensis. Data shown are the mean of 23 temperature response curves collected with error bars representing ± 2 standard deviation.

152x153mm (300 x 300 DPI)

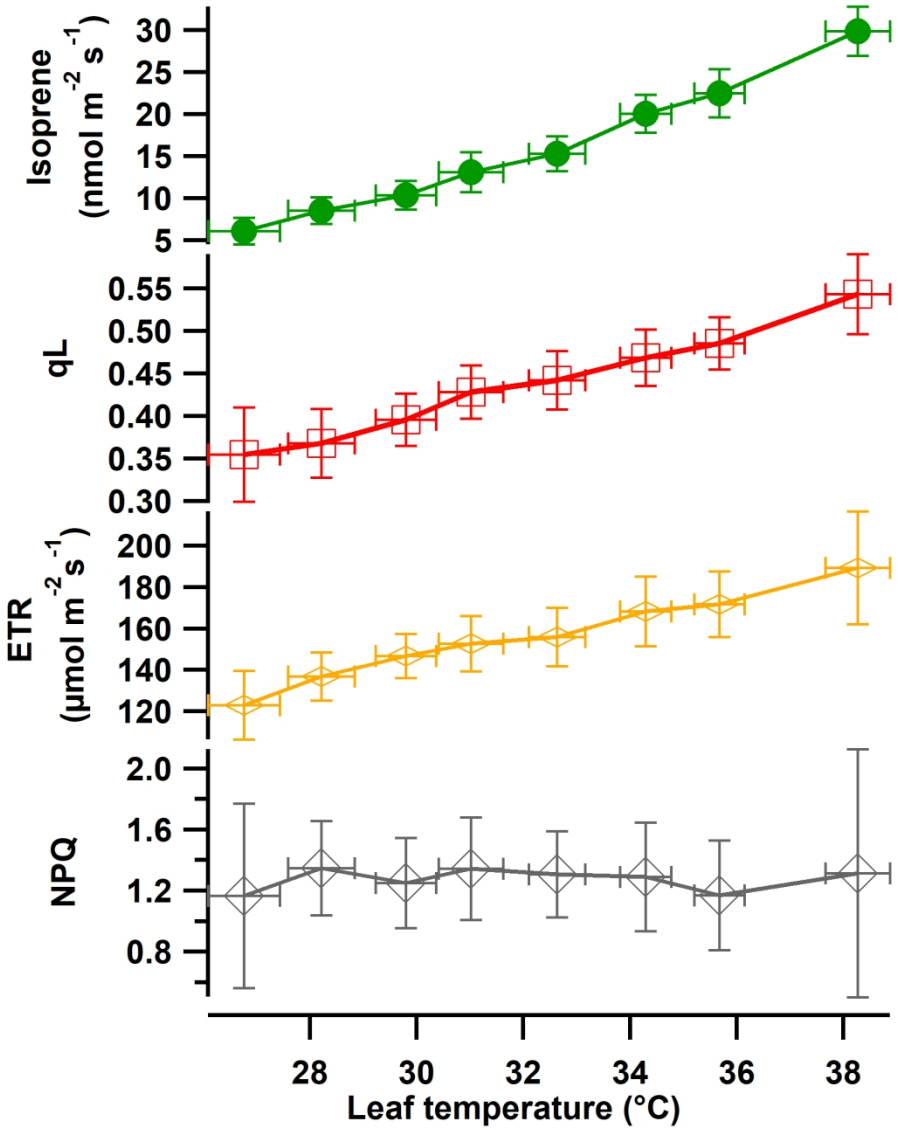


Figure 2: Mean *V. guianensis* leaf temperature responses of light-dependent photosynthetic parameters including electron transfer rate (ETR), oxidation state of QA ($q_L$), and non- photochemical quenching (NPQ) together with leaf isoprene emissions. Data shown are the mean of 23 temperature response curves collected with error bars representing ± 2 standard deviation.

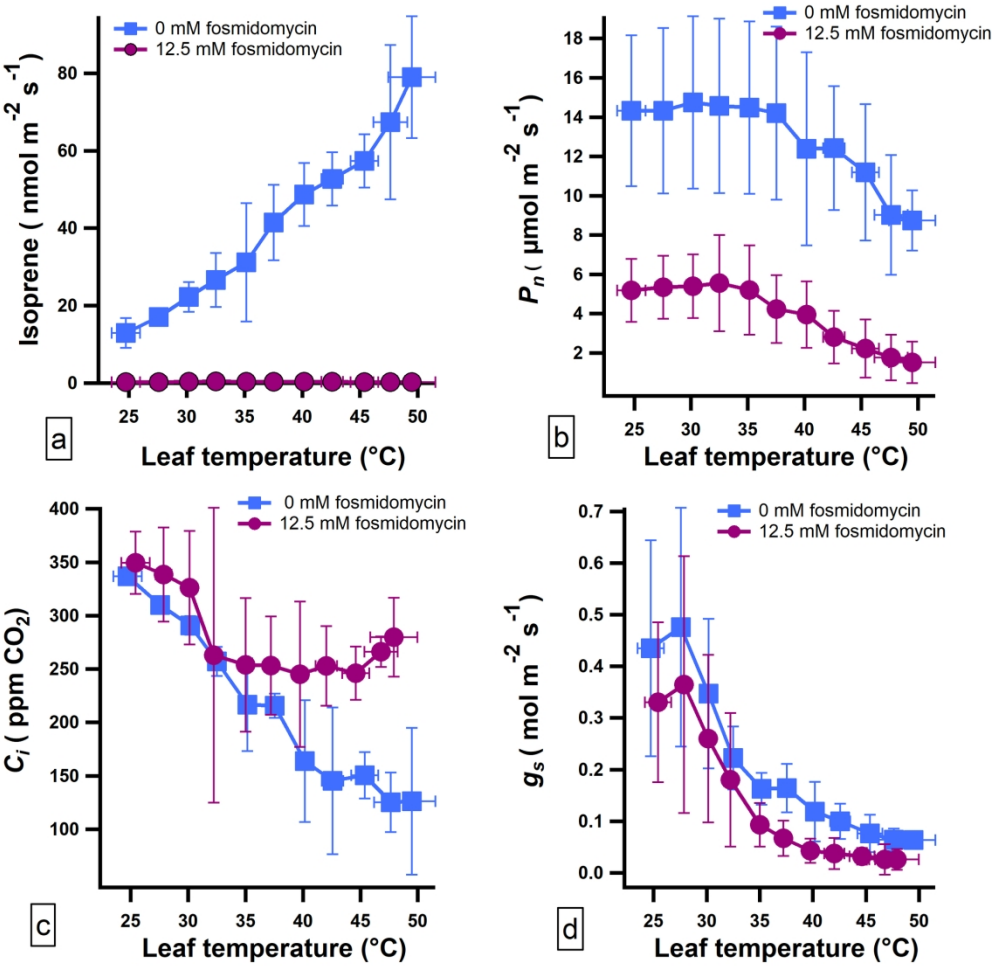


Figure 3: Mean V. guianensis leaf temperature responses after 1 hour of branch feeding with 0 mM (blue curves with squares) and 12.5 mM (purple curves with dots) of the isoprenoid pathway inhibitor fosmidomycin showing (a) isoprene emissions, (b) net photosynthesis, Pn, (c) intercellular CO2 concentration, Ci, (d) stomatal conductance, gs. Data shown are the mean of 3-4 temperature response curves (1 curve per leaf) with error bars representing ± 2 standard deviation.

191x187mm (300 x 300 DPI)

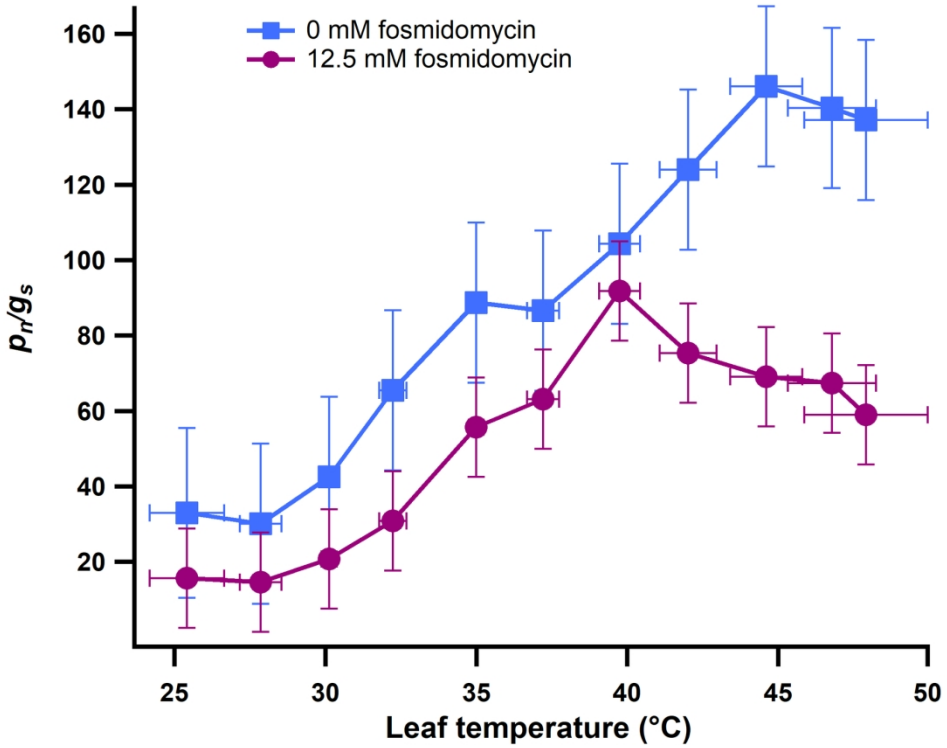


Figure 4: Mean V. guianensis leaf temperature responses after 1 hour of branch feeding with 0 mM (blue curves with squares) and 12.5 mM (purple curves with dots) of the isoprenoid pathway inhibitor fosmidomycin showing net photosynthesis normalized to stomatal conductance, Pn/gs. Data shown are the mean of 3-4 temperature response curves (1 curve per leaf) with error bars representing ± 2 standard deviation.

165x127mm (300 x 300 DPI)

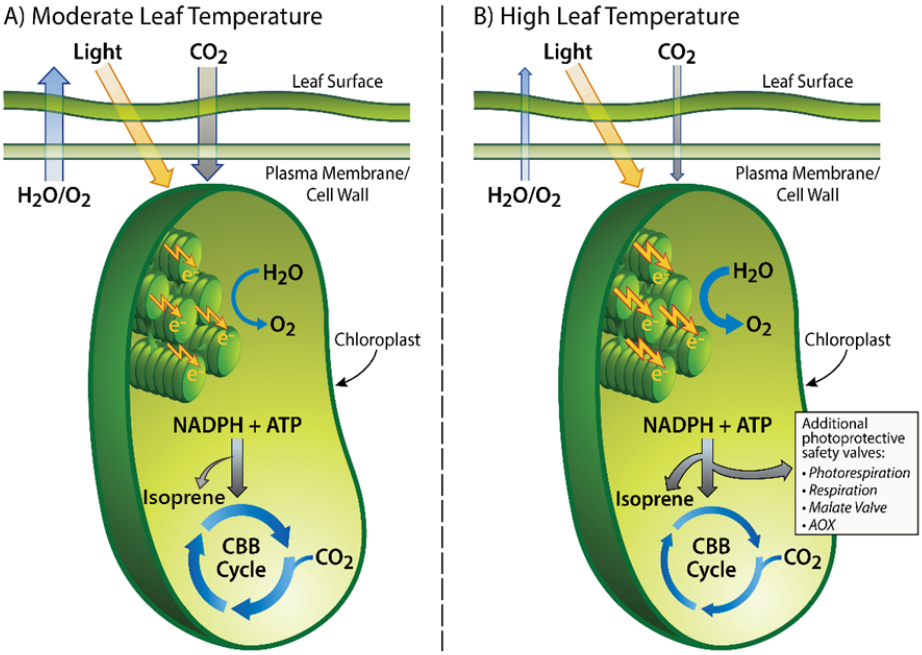


Figure 5: Proposed biochemical model of the acclimation to high temperature stress through the consumption of photosynthetic energy (ATP) and reducing equivalents (NADPH) through the activation of the isoprenoid pathway together in parallel with other coupled biochemical pathways (adapted from Voss *et al*., 2013 and Morfopoulos *et al*., 2014). $O_2$: oxygen; $CO_2$: carbon dioxide; $H_2O$: water; ATP: adenosine triphosphate; NADPH: Nicotinamide-Adenine-Dinucleotide-Phosphate; AOX: alternative oxidases of mitochondria.

254x190mm (96 x 96 DPI)